

Nambu-Covariant Many-Body Theory I: Perturbative Approximations

M. Drissi ^{1,*} A. Rios ^{1,2} and C. Barbieri ^{3,4,1}

¹*Department of Physics, University of Surrey, Guildford GU2 7XH, United Kingdom*

²*Departament de Física Quàntica i Astrofísica, Institut de Ciències del Cosmos (ICCUB),
Universitat de Barcelona, Martí Franquès 1, E08028 Barcelona, Spain*

³*Dipartimento di Fisica, Università degli Studi di Milano, Via Celoria, 16, I-20133 Milano, Italy*

⁴*INFN, Sezione di Milano, Via Celoria 16, I-20133 Milano, Italy*

(Dated: September 7, 2021)

Symmetry-breaking considerations play an important role in allowing reliable and accurate predictions of complex systems in quantum many-body simulations. The general theory of perturbations in symmetry-breaking phases is nonetheless intrinsically more involved than in the unbroken phase due to non-vanishing anomalous Green's functions or anomalous quasiparticle interactions. In the present paper, we develop a formulation of many-body theory at non-zero temperature which is explicitly covariant with respect to a group containing Bogoliubov transformations. Based on the concept of Nambu tensors, we derive a factorisation of standard Feynman diagrams that is valid for a general Hamiltonian. The resulting factorised amplitudes are indexed over the set of un-oriented Feynman diagrams with fully antisymmetric vertices. We argue that, within this framework, the design of symmetry-breaking many-body approximations is simplified.

I. INTRODUCTION

Modern descriptions of complex quantum physical systems are largely based on their decomposition in a set of idealised sub-parts or particles. The correlations between the individual motion of these particles are usually described in terms of so-called many-body interactions, obtained by subtracting the Hamiltonian of free particles from the Hamiltonian describing the targeted complex quantum physical system. The quantum theory of many-body systems provides tools to perform this decomposition conveniently for a wide variety of particles, together with means of computing their correlations and associated many-body observables, whether approximately or exactly. How to conveniently devise many-body approximations when there is a mismatch between the symmetries of the free system and those of the correlated many-body system? This is a key question in quantum many-body theory which we aim to addressing in the present paper.

Since the work of Bardeen, Cooper and Schrieffer (BCS) [1, 2], the theory of perturbations over a reference state breaking particle-number symmetry has been formulated in several ways [3–6]. Shortly after the developments of the BCS theory, Bogoliubov [3] and Valatin [7] showed it to be equivalent to a reformulation of many-body theory in terms of quasiparticle creation and annihilation operators breaking particle-number symmetry. The need for anomalous vertices in the associated perturbation theory was immediately recognised [3, 8, 9]. Soon after, Gorkov emphasised that one could keep working with traditional single-particle creation and annihilation operators to the price of introducing anomalous Green's functions [4]. This amounts to exchanging the complexity associated to anomalous vertices with the one associated

to anomalous lines in the diagrammatics of perturbation theory. Slightly later, Anderson pinpointed a two dimensional space structure as a useful organising principle to mitigate the growing complexity due to the occurrence of anomalous contributions [10]. Nambu took this idea further and reformulated the many-body problem in terms of the so-called Nambu fields [11]. These extended fields respect the usual canonical anticommutation rules, and standard perturbation theory can be applied straightforwardly. The result is an oriented diagrammatic approach, free of anomalous lines, where propagators are 2×2 matrices. We refer the reader to Chap. 15 of Ref. [12] for more details on the oriented diagrammatics in the formalism of Nambu. Among subsequent developments in diagrammatic approaches dealing explicitly with symmetry-breaking, we highlight here the pioneering work by De Dominicis and Martin on superfluidity [13, 14]. In their work, perturbative contributions were expressed in terms of diagrams with un-oriented lines and totally antisymmetric vertices so that any further development is simplified. Later, a similar formalism was reintroduced by Kleinert, in his work on collective excitations [15, 16], as well as by Haussmann, in his work on the BCS-BEC crossover [17, 18]. In this context, the present work can be seen as rooting the specific formalisms developed in [13–18] into the formalism of Nambu tensors, thus extending them to the case of a general Hamiltonian expressed in a general extended basis.

Dealing with symmetry-breaking, whether realised explicitly or spontaneously, has been understood to be essential in the description of physical phenomena for more than a century [19, 20]. In practice, those considerations are of importance to efficiently produce accurate and reliable predictions of a wide range of physical phenomena. Symmetry breaking has been identified not only in BCS electron superconductors, but also in superfluid helium; in the BCS-BEC crossover of ultracold atoms or in exciton physics. Nuclear systems are iconic in this respect. Theo-

* m.drissi@surrey.ac.uk

retical descriptions of nuclei regularly break the symmetries of translation, rotation and particle number [21]. In the case of infinite homogeneous nuclear matter, the reliability of *ab initio* theoretical predictions are of paramount importance for neutron-star modelling [22, 23].

The main physics motivation behind the formal developments presented here is the description of nuclear systems and particularly of superfluid neutron matter. For the last 50 years, Hartree-Fock-Bogoliubov (HFB) calculations, or their extensions, have predicted superfluid gaps with a fluctuating magnitude depending on the inter-nucleonic interaction and on the additional many-body corrections taken into account [23–32]. For example, the question of whether a 3PF_2 gap contributes significantly to the structure and dynamics of homogeneous neutron matter, and if so at what densities and temperatures, is still an open problem [27, 33]. Simultaneously, some models of neutron star cooling have shown a better agreement with observations when assuming the 3PF_2 gap to be small enough [33–36]. The potential tension between neutron star cooling observations and *ab initio* nuclear estimates of the superfluid pairing gaps signals the need for clear and quantifiable predictions of the phase diagram of homogeneous neutron matter.

This goal requires developing an approach that can be used to estimate many-body corrections, similarly to what is done routinely in the normal phase [37–40]. Ideally, one would also like to be able to include non-perturbative diagrammatic summations in the description, to quantify and clarify the importance of the so-called screening corrections, one of the longstanding issues in the field [28, 41]. For nuclear physics applications at high densities, two-, but also three- and higher-body interactions, need to be considered. Finally, the approach should be formulated at non-zero temperature, to explore the complete phase diagram extensively.

One possibility along these lines would be to start from HFB computations at non-zero temperature and use previously existing diagrammatic methods to treat the spontaneous breaking of particle-number symmetry beyond mean-field. Similar approaches have proved very effective for finite nuclei [42, 43]. However, devising high-accuracy approximations with two- and three-body interactions becomes increasingly difficult already at zero temperature and in the absence of any degeneracy [44–46]. Perturbative diagrammatic approaches in the symmetry-breaking case are even more cumbersome (and hence error-prone) than their symmetry-conserving counterparts. Such complications become increasingly relevant if one aims at describing not one single observable (say, the energy), but rather the equilibrium dynamics of the system through many-body Green’s functions. Some of this complexity has been addressed by means of automated diagrammatic generation tools [39, 47–49]. While these are useful for avoiding redundant derivations, automated frameworks fall short when one is interested in summing an infinite set of Feynman diagrams and further developments are required for each type of diagrammatic summation. For

example, many-body approximations based on Gorkov self-consistent Green’s functions [5, 50], Bogoliubov coupled cluster [6, 51] or random-phase approximations [10] sum specific sets of infinite diagrams in a particle-number symmetry-broken phase.

To tackle this recurrent problem, we introduce a reformulation of the quantum many-body problem in the present paper. The present work can be seen as the natural continuation of the pioneering work of De Dominicis and Martin [13, 14], Kleinert [15, 16] and Haussmann [17, 18]. These developments provided a solid starting point but also introduced restrictive hypotheses, either on the choice of the working basis or the type of interaction, to simplify some formal steps. The success of the previous formalisms are shown to be underpinned by the algebraic structure of Nambu tensors which we introduce in the present paper as an extension of the standard single-particle tensor algebra [52, 53]. This allows us to lift the previous restrictive hypotheses, thus extending previous developments to the case of a generic Hamiltonian expressed in an unrestricted extended basis. The resulting Nambu-covariant formalism has a natural diagrammatic representation in terms of un-oriented Feynman diagrams¹. A key difference with respect to more standard approaches is the introduction of fully antisymmetric interaction vertices. We show that each un-oriented Feynman diagram factorises a sum of standard (e.g. Gorkov) Feynman diagrams with anomalous propagators and vertices. Moreover, the approach provides a perturbative expansion of many-body Green’s functions in terms of Nambu tensors that are, in particular, contravariant with respect to Bogoliubov transformations. For future references, we refer to this formulation of perturbation theory as Nambu-Covariant Perturbation Theory (NCPT). Whereas here we focus mainly on NCPT, we analyse the properties of (self-consistent) Green’s functions and provide formal developments for summation schemes in a follow-up publication, hereafter referred to as Part II [54].

The advantages of the Nambu-covariant reformulation, compared to more standard approaches, are threefold. First, we win clarity on formal aspects. The exact properties of many-body Green’s functions and other amplitudes associated to un-oriented Feynman diagrams can be expressed in a more compact, less cumbersome manner. At a given order of perturbation theory, the number of un-oriented Feynman diagrams is also substantially reduced compared to other approaches, thus mitigating as much as possible the factorial growth in diagram number. In turn, the resulting formalism is less error-prone. Moreover, any many-body approximation obtained as a truncation on the set of un-oriented Feynman diagrams is guaranteed to be independent from the extended basis that is necessary

¹ Throughout this work, we use “un-oriented” to specify Feynman diagrams defined with plain lines, i.e. without any line orientation.

for practical implementations. In other words, there is no need for a re-derivation of many-body equations when working with two different extended bases related by a Bogoliubov transformation. We expect that these formal results should be useful in numerical implementations and associated benchmarking tests.

Second, on numerical aspects, we expect the numerical code resulting from a direct implementation of formulae expressed in the Nambu-covariant formalism to be more computationally efficient than previous attempts. The formalism provides compact and factorised expressions, thus facilitating the implementation and the maintenance of source codes. As we discuss later, from a computational efficiency perspective, the equations derived in this formalism expose more clearly a source of parallelisation. The formalism reduces the number of Feynman diagrams whose evaluation transparently translates into a Nambu tensor network. Compared to the evaluation of a multitude of single-particle tensor networks, we expect a greater gain when using massively parallel hardware with algorithms specifically designed for this kind of architecture [55, 56].

Last, we stress that the Nambu-covariant formalism may also be useful in the development of automated pipelines. The formalism does not only reduce the number of diagrams, which would no doubt speed up automated diagrammatic generation tools, but also removes any consideration in terms of orientations. We expect this to bring a substantial advantage in terms of memory processing and practical implementation.

The formalism developed in this paper is entirely equivalent to any of the previous formulations. In principle, a perfectly efficient numerical implementation might not benefit from it. Similarly, fully factorised and simplified formal many-body equations can also be derived in existing formalisms. Our claim is, however, that the Nambu-covariant formalism presented here provides a key to uncover sources of formal simplifications and generalisations. We also expect it will lead to new numerical optimisations in the implementation of many-body approximations. Hopefully, this formalism can benefit other many-body practitioners. In this paper, we present the key aspects of the Nambu-covariant formalism and its application to perturbation theory. In Part II, we will discuss the application of the Nambu-covariant formalism to many-body approximations based on self-consistently dressed propagators and vertices.

This paper is organised as follows. We introduce the essential ideas of Nambu tensors and their relation to Bogoliubov transformations in Sec. II. The resulting NCPT, manifestly covariant with respect to Bogoliubov transformations, is then discussed in Sec. III. We define many-body Green's functions as Nambu tensors and explore their expansion in terms of un-oriented Feynman diagrams. We provide explicit Feynman rules for the time and energy representations, and give an additional set of diagrammatic rules to perform Matsubara sums. In Sec. IV, we explicitly show the connection of this approach

to previously existing formalisms, namely the Gorkov [5] and Bogoliubov [6] ones. Finally, we summarise the key points in Sec. V, where we also provide an outlook of future works.

II. NAMBU TENSOR ALGEBRA

In this section, we introduce the notations that underpin the Nambu-covariant formalism. We discuss Nambu fields and define general Nambu tensors in terms of their transformation properties under a general change of basis. We provide illustrative examples of such tensors at the end of this section.

A. Definitions

We consider a many-body system of fermions. The Fock space \mathcal{F} of the many-fermion system is spanned by the tensor products of a one-body Hilbert space \mathcal{H}_1 of the states of a single fermion. Let us define a basis $\mathcal{B} \equiv \{|b\rangle\}$ of \mathcal{H}_1 . Indices b, c, \dots are used to denote states within \mathcal{B} .

Since we do not assume the basis to be orthogonal, it is convenient to introduce the associated dual basis $\bar{\mathcal{B}} \equiv \{\langle \bar{b} | \}$ such that \mathcal{B} and $\bar{\mathcal{B}}$ verify the biorthogonality condition

$$\langle \bar{b} | c \rangle = \delta_{bc} , \quad (1)$$

where δ_{bc} denotes the usual Kronecker symbol. The dual space of \mathcal{H}_1 is denoted as \mathcal{H}_1^\dagger . For any basis \mathcal{B} of \mathcal{H}_1 , we define the Hermitian conjugated basis $\mathcal{B}^\dagger \equiv \{\langle b | \}$ of \mathcal{H}_1^\dagger . In the special case where \mathcal{B} is orthonormal, we have $\bar{\mathcal{B}} = \mathcal{B}^\dagger$.

The creation and annihilation operators associated to \mathcal{B} are denoted as \bar{a}_b and a_b , respectively. Here, we chose the bar notation used in Ref. [57] for the dual basis². We stress that, in general, $\bar{a}_b = a_b^\dagger \neq a_b^\dagger$ [57]. Creation and annihilation operators verify the canonical anticommutation relations

$$\{\bar{a}_b, \bar{a}_c\} = 0 , \quad (2a)$$

$$\{a_b, a_c\} = 0 , \quad (2b)$$

$$\{\bar{a}_b, a_c\} = \delta_{bc} . \quad (2c)$$

At this point, considering tensors over \mathcal{H}_1 and \mathcal{H}_1^\dagger would give us the standard single-particle tensor algebra, which has been studied and applied in the context of quantum chemistry in Refs. [52, 53]. For instance, let us consider the tensor product space $\mathcal{H}_1^{\otimes p} \otimes (\mathcal{H}_1^\dagger)^{\otimes q}$

² Note that alternative notations exist such, as the one used in Refs. [52, 53].

of type (p, q) single-particle tensors. A change of single-particle basis modifies the coordinates of a type (p, q) single-particle tensor according to the standard tensor product representation of the linear group $\text{GL}(\mathcal{H}_1)$. If we consider the Fock space, the associated representation of $\text{GL}(\mathcal{H}_1)$ characterising a change of single-particle basis can be decomposed in the sum of representations over the N -body Hilbert space $\mathcal{H}_N \equiv \mathcal{H}_1^{\otimes N}$. This is a consequence of the stability of \mathcal{H}_N with respect to a change of single-particle basis. For example, if t_{bc} are the components of an element of \mathcal{H}_2 (i.e. of a $(2, 0)$ single-particle tensor), and U is the invertible matrix representing a change of single-particle basis, the new components after changing the single-particle basis read

$$t'_{bc} \equiv \sum_{de} U_{bd}^{-1} U_{ce}^{-1} t_{de} . \quad (3)$$

In practice, working with tensors over $\text{GL}(\mathcal{H}_1)$ allows one to keep track of how a change of single-particle basis affects a set of components. Tensors also provide a powerful organising tool to classify contributions to observables, which must necessarily be invariant with respect to a change of single-particle basis. Tensorial considerations can also be used to guide physically motivated approximations [52, 53]. Unfortunately, the practical advantages of single-particle tensor algebra cannot be carried over to the larger group of linear canonical transformations, namely Bogoliubov transformations [58]. In particular, the sub-spaces \mathcal{H}_N are no longer stable with respect to (the group of) Bogoliubov transformations.

We explore here a more convenient tensor algebra that arises at the price of extending \mathcal{H}_1 to a vector space of double dimension. Such a doubled-dimension vector space was already introduced in the work of Anderson [10] and Nambu [11] on symmetry-broken systems. This extended one-body Hilbert space, \mathcal{H}_1^e , is defined as the product of the original one-body space and its dual,

$$\mathcal{H}_1^e \equiv \mathcal{H}_1 \times \mathcal{H}_1^\dagger . \quad (4)$$

We define the extended basis \mathcal{B}^e of \mathcal{H}_1^e as

$$\mathcal{B}^e \equiv \mathcal{B} \cup \bar{\mathcal{B}} , \quad (5)$$

where the basis \mathcal{B} of \mathcal{H}_1 and $\bar{\mathcal{B}}$ of \mathcal{H}_1^\dagger are to be understood as the free families $\mathcal{B} \times \{0\}$ and $\{0\} \times \bar{\mathcal{B}}$, respectively. Elements of \mathcal{H}_1^e are vectors of the form

$$\begin{pmatrix} |\Psi_1\rangle \\ \langle \Psi'_1| \end{pmatrix} . \quad (6)$$

This extended one-body Hilbert space is equipped with the inner product $g(\cdot, \cdot)$, defined as

$$g \left(\begin{pmatrix} |\Psi_1\rangle \\ \langle \Psi'_1| \end{pmatrix}, \begin{pmatrix} |\Psi_2\rangle \\ \langle \Psi'_2| \end{pmatrix} \right) \equiv \langle \Psi'_2 | \Psi_1 \rangle + \langle \Psi'_1 | \Psi_2 \rangle , \quad (7)$$

which is a non-degenerate symmetric \mathbb{C} -bilinear form.

It is convenient to re-index elements of \mathcal{B}^e over a global index $\mu \equiv (b, l)$, where b denotes states in the space \mathcal{H}_1 and $l \in \{1, 2\}$ is a Nambu index. This index labels a state of \mathcal{B} ($l = 1$) or of $\bar{\mathcal{B}}$ ($l = 2$). We define the involution $\bar{\cdot}$ on the set of Nambu indices l by

$$\begin{aligned} \bar{\cdot} : 1 &\mapsto \bar{1} = 2 \\ 2 &\mapsto \bar{2} = 1 , \end{aligned} \quad (8)$$

and we extend it to global indices $\mu = (b, l)$ by

$$\bar{\mu} \equiv (b, \bar{l}) . \quad (9)$$

Explicitly, vectors $|\mu\rangle$ of \mathcal{B}^e are defined by

$$|b, 1\rangle \equiv \begin{pmatrix} |b\rangle \\ 0 \end{pmatrix} , \quad (10a)$$

$$|b, 2\rangle \equiv \begin{pmatrix} 0 \\ \langle \bar{b}| \end{pmatrix} . \quad (10b)$$

The components of the metric $g_{\mu\nu}$ associated to the tensor algebra generated by the extended one-body Hilbert space \mathcal{H}_1^e are defined by

$$g_{\mu\nu} \equiv g(|\mu\rangle, |\nu\rangle) . \quad (11)$$

In the extended basis \mathcal{B}^e , the metric reads simply

$$g_{\mu\nu} = \delta_{\mu\bar{\nu}} , \quad (12)$$

where $\delta_{\mu\nu}$ is the Kronecker symbol over global indices.

We have so far introduced new global indices in \mathcal{H}_1^e which, together with a new inner product, will be convenient to use when working within the Nambu tensor algebra. Performing an analogous study on the dual of \mathcal{H}_1^e gives us the dual components of the metric, $g^{\mu\nu}$. In the extended basis \mathcal{B}^e , these components read

$$g^{\mu\nu} = \delta_{\mu\bar{\nu}} . \quad (13)$$

Finally, for completeness, we define the mixed components of the metric, $g^{\mu\nu}$ and $g_{\mu\nu}$, by

$$g^{\mu\nu} \equiv \sum_{\lambda} g^{\mu\lambda} g_{\lambda\nu} = \delta_{\mu\nu} , \quad (14)$$

$$g_{\mu\nu} \equiv \sum_{\lambda} g_{\mu\lambda} g^{\lambda\nu} = \delta_{\mu\nu} . \quad (15)$$

Creation and annihilation operators are conveniently grouped in the Nambu fields A^μ and \bar{A}_μ . These are defined such that they read in the extended basis \mathcal{B}^e

$$A^{(b,1)} \equiv a_b , \quad (16a)$$

$$A^{(b,2)} \equiv \bar{a}_b , \quad (16b)$$

$$\bar{A}_{(b,1)} \equiv \bar{a}_b , \quad (16c)$$

$$\bar{A}_{(b,2)} \equiv a_b . \quad (16d)$$

Just as in standard tensor algebra, indices in the Nambu fields can be raised and lowered using the metric

$$\bar{A}_\mu = \sum_\nu g_{\mu\nu} A^\nu, \quad (17a)$$

$$\bar{A}_\mu = \sum_\nu g_\mu{}^\nu \bar{A}_\nu, \quad (17b)$$

$$A^\mu = \sum_\nu g^{\mu\nu} \bar{A}_\nu, \quad (17c)$$

$$A^\mu = \sum_\nu g^\mu{}_\nu A^\nu. \quad (17d)$$

The canonical anticommutation rules read

$$\{A^\mu, A^\nu\} = g^{\mu\nu}, \quad (18a)$$

$$\{A^\mu, \bar{A}_\nu\} = g^\mu{}_\nu, \quad (18b)$$

$$\{\bar{A}_\mu, A^\nu\} = g_\mu{}^\nu, \quad (18c)$$

$$\{\bar{A}_\mu, \bar{A}_\nu\} = g_{\mu\nu}. \quad (18d)$$

These expressions indicate that the Nambu formalism is underpinned by an implicit tensor algebra structure. We stress that, although the metric and Nambu fields expressed in \mathcal{B}^e are quite simple, this is no longer the case in a general extended basis of \mathcal{H}_1^e . The specific notation $g_{\mu\nu}$ and A^μ will be particularly useful. Next, we make explicit the resulting algebra of so-called Nambu tensors and we relate it to the group of Bogoliubov transformations.

B. Nambu tensors

Nambu tensors are defined as elements of the tensor algebra $T(\mathcal{H}_1^e)$ built over the vector space \mathcal{H}_1^e . Intrinsically, i.e. without mentioning any basis, a Nambu tensor t of type (p, q) is a multilinear form over p times the Cartesian product of \mathcal{H}_1^e and q times its dual. Equivalently, one can work directly on the coordinates of a Nambu (p, q) -tensor t , which are written as

$$t^{\mu_1 \dots \mu_p}{}_{\nu_1 \dots \nu_q}. \quad (19)$$

For these coordinates to be a (p, q) type Nambu tensor, they must transform according to the standard tensor product representation of $\text{GL}(\mathcal{H}_1^e)$ on $T(\mathcal{H}_1^e)$. In other words, when changing basis, the new coordinates must read

$$\begin{aligned} t^{\mu_1 \dots \mu_p}{}_{\nu_1 \dots \nu_q} &\equiv \\ &\sum_{\substack{\lambda_1 \dots \lambda_p \\ \kappa_1 \dots \kappa_q}} (\mathcal{W}^{-1})^{\mu_1}{}_{\lambda_1} \dots (\mathcal{W}^{-1})^{\mu_p}{}_{\lambda_p} \\ &\times t^{\lambda_1 \dots \lambda_p}{}_{\kappa_1 \dots \kappa_q} \mathcal{W}^{\kappa_1}{}_{\nu_1} \dots \mathcal{W}^{\kappa_q}{}_{\nu_q}, \quad (20) \end{aligned}$$

where \mathcal{W} is an invertible matrix representing the change of basis of \mathcal{H}_1^e .

Nambu tensors, as defined above, are of great use when considering general Bogoliubov transformations. A Bogoliubov change of basis of the Fock space \mathcal{F} is equivalent

to a linear transformation of Nambu fields [57]. In other words, a Nambu field transforms according to

$$A'^\mu = \sum_\nu (\mathcal{W}^{-1})^\mu{}_\nu A^\nu, \quad (21a)$$

$$\bar{A}'_\mu = \sum_\nu \mathcal{W}^\nu{}_\mu \bar{A}_\nu, \quad (21b)$$

where A'^μ and \bar{A}'_μ are the new Nambu fields³ and $\mathcal{W}^\mu{}_\nu$ are the elements of a g -orthogonal matrix that verifies

$$\sum_{\lambda\kappa} g_{\lambda\kappa} \mathcal{W}^\lambda{}_\mu \mathcal{W}^\kappa{}_\nu = g_{\mu\nu}. \quad (22)$$

This g -orthogonality condition is equivalent to restricting linear transformations of Nambu fields to those conserving the canonical anticommutation rules in Eqs. (18).

Mathematically speaking, the group of Bogoliubov changes of basis of \mathcal{F} is isomorphic to the orthogonal group $\text{O}(\mathcal{H}_1^e, g)$, namely the group of basis changes of \mathcal{H}_1^e preserving the inner product g defined in Eq. (7). The effect of a Bogoliubov change of basis of \mathcal{F} on Nambu tensors is represented by the standard tensor product representation of $\text{O}(\mathcal{H}_1^e, g)$ on $T(\mathcal{H}_1^e)$. In particular, the spaces of (p, q) -Nambu tensors are stable with respect to that action and their coordinates transform as in Eq. (20) but with \mathcal{W} a matrix that now characterises the Bogoliubov transformation. Similarly, the effect of a single-particle change of basis of \mathcal{F} on Nambu tensors is represented by the standard tensor product representation of $\text{GL}(\mathcal{H}_1)$ on $T(\mathcal{H}_1^e)$.

As it is common in the theory of tensor algebra, a Nambu (p, q) -tensor will be said to have p contravariant and q covariant indices. Contravariant and covariant indices are respectively represented by upper and lower indices. We note that covariance (contravariance) is here to be understood with respect to a change of basis of \mathcal{H}_1^e . Since

$$\text{GL}(\mathcal{H}_1) \subset \text{O}(\mathcal{H}_1^e, g) \subset \text{GL}(\mathcal{H}_1^e), \quad (23)$$

the covariance (contravariance) remains valid for single-particle and Bogoliubov transformations. Let us stress that $\text{GL}(\mathcal{H}_1^e)$ also contains non-canonical transformations which modify the components of the metric $g_{\mu\nu}$ i.e. the inclusions in Eq. (23) are strict. An example of such transformation will be discussed in Sec. IV.

Whenever there is possible ambiguity, we refer to single-particle, Bogoliubov and Nambu covariance (contravariance) to distinguish between the specific group of transformations. In the remainder of this work, we will be mostly concerned with Nambu tensors of a certain type. We stress that such tensors are the cornerstone allowing us to easily prove our equations to be either contravariant or covariant with respect to $\text{GL}(\mathcal{H}_1^e)$ and, as a sub-case, to any Bogoliubov transformation.

³ Note that in a general extended basis $\mathcal{B}^{e'}$, the Nambu fields are general linear combinations of creation and annihilation operators, unlike the specific case given in Eqs. (16).

C. Elementary examples

Having defined Nambu tensors formally in the previous subsection, we now provide a series of illustrative examples. We focus on practical applications of Nambu tensor algebra, which pave the way for the formal and diagrammatic developments that follow.

1. Basic Nambu tensors

We start by looking at a key tensor, the metric. We have so far introduced four metric objects, i.e. $g^{\mu\nu}$, $g^\mu{}_\nu$, $g_\mu{}^\nu$ and $g_{\mu\nu}$. In our notation, these represent the coordinates of tensors of type $(2,0)$, $(1,1)$, $(1,1)$ and $(0,2)$, respectively. Similarly to other tensor algebras, basis transformations can also be describe as tensors. The matrix elements of a change of extended basis, $\mathcal{W}^\mu{}_\nu$, can be considered as the coordinates of a $(1,1)$ -tensor.

We now consider an arbitrary k -body operator, O in terms of Nambu tensors. O can be represented by a (p,q) -tensor, so long as $p+q=2k$. For instance, in the case where $p=k$ and $q=k$, the mixed (k,k) representation of O reads

$$O \equiv \sum_{\substack{\mu_1 \dots \mu_k \\ \nu_1 \dots \nu_k}} o^{\mu_1 \dots \mu_k}{}_{\nu_1 \dots \nu_k} \bar{A}_{\mu_1} \dots \bar{A}_{\mu_k} A^{\nu_1} \dots A^{\nu_k} , \quad (24)$$

where $o^{\mu_1 \dots \mu_k}{}_{\nu_1 \dots \nu_k}$ are the coordinates of a (k,k) -tensor. Equivalently, a fully covariant representation of the same operator O reads

$$O \equiv \sum_{\mu_1 \dots \mu_{2k}} o_{\mu_1 \dots \mu_{2k}} A^{\mu_1} \dots A^{\mu_{2k}} , \quad (25)$$

where $o_{\mu_1 \dots \mu_{2k}}$ are now the coordinates of a $(0,2k)$ -tensor. Finally, the fully contravariant representation reads

$$O \equiv \sum_{\mu_1 \dots \mu_{2k}} o^{\mu_1 \dots \mu_{2k}} \bar{A}_{\mu_1} \dots \bar{A}_{\mu_{2k}} , \quad (26)$$

where $o^{\mu_1 \dots \mu_{2k}}$ are coordinates of a $(2k,0)$ -tensor. We can use the index raising and lowering operations in Eqs. (17) to relate the coordinates of the different types of tensors,

$$o_{\mu_1 \dots \mu_{2k}} = \sum_{\alpha_1 \dots \alpha_k} g_{\mu_1 \alpha_1} \dots g_{\mu_k \alpha_k} o^{\alpha_1 \dots \alpha_k}{}_{\mu_{k+1} \dots \mu_{2k}} , \quad (27a)$$

$$o^{\mu_1 \dots \mu_{2k}} = \sum_{\alpha_1 \dots \alpha_k} o^{\mu_1 \dots \mu_k}{}_{\alpha_1 \dots \alpha_k} g^{\alpha_1 \mu_{k+1}} \dots g^{\alpha_k \mu_{2k}} . \quad (27b)$$

2. Building new Nambu tensors

We now turn our attention to a series of additional tensor operations that will be necessary in our derivations. In particular, we discuss here transpositions, linear combinations, tensor products and tensor contractions.

Let us first start with transpositions, which essentially correspond to a different reordering of the indices. For example, in the case of the $(1,1)$ - and $(0,2)$ -tensors of coordinates $t^\mu{}_\nu$ and $s_{\mu\nu}$, the only possible transpositions read:

$$(t^\Gamma)^\nu{}_\mu \equiv t^\nu{}_\mu , \quad (28a)$$

$$(s^\Gamma)_{\mu\nu} \equiv s_{\nu\mu} . \quad (28b)$$

Note that the contravariant or covariant character of the indices is kept by transpositions. Using this transposition together with the raising and lowering of indices given in Eqs. (27), the g-orthogonality condition in Eq. (22) reads simply,

$$\sum_\lambda (\mathcal{W}^\Gamma)^\mu{}_\lambda \mathcal{W}^\lambda{}_\nu = g^\mu{}_\nu . \quad (29)$$

We now turn our attention to linear combinations. The space of tensors of a fixed type is a vector space. As such, tensors of the same type can be linearly combined while keeping the tensorial structure intact. For example, the (anti)symmetrisation of a tensor gives back a tensor of the same type. We note, however, that contravariant and covariant indices must be (anti)symmetrised separately. Consider, for instance, the coordinates

$$o^{[\mu_1 \dots \mu_k]}{}_{(\nu_1 \dots \nu_k)} , \quad (30)$$

which define a new (k,k) -tensor based on the original components of Eq. (24). The bracketed indices correspond to the shorthand notations for (anti)symmetrisation

$$t_{[\mu_1 \dots \mu_p] \mu_{p+1} \dots} \equiv \frac{1}{p!} \sum_{\sigma \in S_p} \epsilon(\sigma) t_{\mu_{\sigma(1)} \dots \mu_{\sigma(p)} \mu_{p+1} \dots} , \quad (31)$$

$$t_{(\mu_1 \dots \mu_p) \mu_{p+1} \dots} \equiv \frac{1}{p!} \sum_{\sigma \in S_p} t_{\mu_{\sigma(1)} \dots \mu_{\sigma(p)} \mu_{p+1} \dots} , \quad (32)$$

where S_p is the symmetric group of order p and $\epsilon(\sigma)$ the signature of the permutation σ . Eq. (30) thus corresponds to a new (k,k) tensor which is (anti)symmetric in its (contravariant) covariant indices. In contrast, if t is a $(1,1)$ -tensor, the quantity

$$\frac{t^\mu{}_\nu + t^\nu{}_\mu}{2} \quad (33)$$

does *not* define a new tensor. The ν index is covariant in the first term but contravariant in the second one. As a result, the sum of both behaves neither covariantly nor contravariantly with respect to a change of extended basis.

Finally, new tensors can also be built via tensor networks, i.e. via a combination of tensor products and tensor contractions of previously existing tensors. For example, let $t^{\mu_1 \nu_1}$ and $s_{\mu_2 \nu_2}$ be the coordinates of two tensors of type $(0,2)$ and $(1,1)$, respectively. The coordinates of their tensor product

$$r^{\mu_1 \nu_1}{}_{\mu_2 \nu_2} \equiv t^{\mu_1 \nu_1} s_{\mu_2 \nu_2} \quad (34)$$

define a tensor of type (3, 1). The contraction of the two original tensors, instead, can be defined as

$$r'^{\mu_1\nu_2} \equiv \sum_{\lambda} t^{\mu_1\lambda} s_{\lambda}^{\nu_2}, \quad (35)$$

and yields coordinates of a tensor of type (2, 0).

In the following, most derivations will start from tensors obtained from a set of operators. New tensors will be built by applying transpositions, linear combinations or tensor networks. Ultimately, observables will necessarily be (0, 0)-tensors, insuring Nambu invariance. In standard many-body perturbation theory, theoretical predictions are independent of the choice of the single-particle basis of \mathcal{H}_1 . In the NCPT developed in Sec. III, this independence of theoretical predictions is extended to the choice of basis of \mathcal{H}_1^e . The latter includes Bogoliubov transformations as a sub-case.

D. Quadratic Hamiltonian

As a first concrete example, let us relate the standard expression of a quadratic Hamiltonian to its fully covariant representation. For a given choice of single-particle basis \mathcal{B} , a quadratic Hamiltonian Ω_0 reads, in general,

$$\Omega_0 \equiv \frac{1}{2} \sum_{bc} U_{bc}^{11} \bar{a}_b a_c + U_{bc}^{22} a_b \bar{a}_c + U_{bc}^{12} \bar{a}_b \bar{a}_c + U_{bc}^{21} a_b a_c, \quad (36)$$

where $U_{bc}^{l_b l_c}$ are generic complex numbers. Let us emphasise that we are not requiring Ω_0 to be Hermitian. In terms of type (1, 1)- or (0, 2)-tensors, U^{μ}_{ν} or $U_{\mu\nu}$, Ω_0 reads respectively:

$$\Omega_0 = \frac{1}{2} \sum_{\mu\nu} U^{\mu}_{\nu} \bar{A}_{\mu} A^{\nu}, \quad (37a)$$

$$\Omega_0 = \frac{1}{2} \sum_{\mu\nu} U_{\mu\nu} A^{\mu} A^{\nu}. \quad (37b)$$

Conveniently, we choose our Nambu fields to be related to the same single-particle basis \mathcal{B} , i.e. we choose to work in the extended basis $\mathcal{B}^e = \mathcal{B} \cup \bar{\mathcal{B}}$. In this instance, U^{μ}_{ν} , $U_{\mu\nu}$ and $U_{bc}^{l_b l_c}$ are related according to

$$U^{(b, l_b)}_{(c, l_c)} = U_{bc}^{l_b l_c}, \quad (38)$$

$$U_{(b, l_b)(c, l_c)} = U_{bc}^{\bar{l}_b \bar{l}_c}, \quad (39)$$

where we have used $U_{\mu\nu} = \sum_{\lambda} g_{\mu\lambda} U^{\lambda}_{\nu}$, from Eq. (27a), and $\mu \equiv (b, l_b)$ and $\nu \equiv (c, l_c)$.

Now that $U_{\mu\nu}$ has been related to traditional matrix elements $U_{bc}^{l_b l_c}$, let us specify the symmetry properties of $U_{\mu\nu}$. Decomposing $U_{\mu\nu}$ into its symmetric, $U_{(\mu\nu)}$, and antisymmetric, $U_{[\mu\nu]}$, parts, Ω_0 reads

$$\Omega_0 = \frac{1}{4} \sum_{\mu} U^{\mu}_{\mu} + \frac{1}{2} \sum_{\mu\nu} U_{[\mu\nu]} A^{\mu} A^{\nu}, \quad (40)$$

where Eqs. (18a) and (27) have been used. For simplicity, we assume the term proportional to the identity vanishes, i.e. Ω_0 is purely quadratic. This is equivalent to assuming $U_{\mu\nu}$ to be antisymmetric and traceless, namely

$$U_{\mu\nu} = -U_{\nu\mu}, \quad (41a)$$

$$\sum_{\mu} U^{\mu}_{\mu} = 0. \quad (41b)$$

We stress that the antisymmetrisation of $U_{\mu\nu}$ was trivially obtained by working in a fully covariant representation of Ω_0 . We will take full advantage of the generic idea that fully covariant representations can be easily antisymmetrised while keeping their tensor character intact in Sec. III, where fully antisymmetric vertices associated to k -body interactions will be introduced.

Eventually, the relation in Eq. (38) is simple for the reason that we have chosen our extended one-body Hilbert space basis, \mathcal{B}^e , conveniently. Similar relations for k -body operators are described in App. A. One important advantage of the tensor formulation presented in this paper is that, upon truncation, most equations will be independent from the chosen extended basis \mathcal{B}^e . For example, let us assume we want to work in a new extended basis $\mathcal{B}^{e'}$, rather than the original \mathcal{B}^e . In this case, the transformation \mathcal{W} relating $\mathcal{B}^{e'}$ to \mathcal{B}^e can be applied directly on the equations or objects of interest. This is a key advantage of working with Nambu tensors. In the case of a (0, 2)-tensor U defined from a quadratic Hamiltonian, the coordinates in the new extended basis read simply

$$U'_{\mu\nu} = \sum_{\lambda\kappa} U_{\lambda\kappa} \mathcal{W}^{\lambda}_{\mu} \mathcal{W}^{\kappa}_{\nu}. \quad (42)$$

III. NAMBU-COVARIANT PERTURBATION THEORY

The general formalism of Nambu tensors introduced in Sec. II allows us to present the perturbation theory of many-body Green's functions in a Nambu-covariant fashion. We refer to this specific formulation of perturbation theory as NCPT. First, we introduce many-body Green's functions as Nambu tensors. Second, their perturbative expansion is expressed in terms of contributions respecting the associated co- and contravariance, i.e. any perturbative contribution is a tensor of the same type as the Green's function being expanded. These perturbative contributions are shown to be indexed over a set of un-oriented Feynman diagrams obtained by a set of diagrammatic rules, which we describe explicitly. Third, one-particle irreducible (1PI) contributions to the one-body Green's function are given up to third order as an example of the versatility of the formalism.

We consider in this section a physical system of many-fermions at equilibrium. The system is in a statistical ensemble at inverse temperature β , described by the Hamiltonian Ω . This Hamiltonian describes fermionic

interactions as well as the statistical ensemble. For generality, and anticipating applications in nuclear systems, we consider two-, three- and up to k_{\max} -body interactions.

We define the perturbation theory for a partitioning of the Hamiltonian, $\Omega \equiv \Omega_0 + \Omega_1$, where the unperturbed Hamiltonian, Ω_0 , is purely quadratic and non-necessarily Hermitian. In terms of Nambu fields and tensors,

$$\Omega_0 \equiv \frac{1}{2} \sum_{\mu\nu} U_{\mu\nu} A^\mu A^\nu, \quad (43a)$$

$$\Omega_1 \equiv \sum_{k=0}^{k_{\max}} \frac{1}{(2k)!} \sum_{\mu_1 \dots \mu_{2k}} v_{\mu_1 \dots \mu_{2k}}^{(k)} A^{\mu_1} \dots A^{\mu_{2k}}. \quad (43b)$$

Here, and in the following, we use the fully covariant representation of operators and contravariant Nambu fields.

A. Many-body Green's functions

We write the exact and the unperturbed (statistical) density matrices of the system, together with their partition functions, as

$$\rho \equiv \frac{1}{Z} e^{-\beta\Omega}, \quad (44a)$$

$$Z \equiv \text{Tr} (e^{-\beta\Omega}), \quad (44b)$$

$$\rho_0 \equiv \frac{1}{Z_0} e^{-\beta\Omega_0}, \quad (44c)$$

$$Z_0 \equiv \text{Tr} (e^{-\beta\Omega_0}). \quad (44d)$$

We use the notation $\langle \dots \rangle$ and $\langle \dots \rangle_0$ for the ensemble averages with respect to the exact and unperturbed density matrices, respectively. Using the imaginary-time formalism, we define the contravariant k -body Green's function as⁴

$$(-1)^k \mathcal{G}^{\mu_1 \dots \mu_{2k}}(\tau_1, \dots, \tau_{2k}) \equiv \langle \text{T} [A^{\mu_1}(\tau_1) \dots A^{\mu_{2k}}(\tau_{2k})] \rangle, \quad (45)$$

Here, the (imaginary) time evolution depends on the complete Hamiltonian, Ω , and $\text{T}[\dots]$ denotes the time-ordering from right to left when increasing imaginary-time, τ . At any fixed time, the contravariant k -body Green's function is a $(2k, 0)$ -tensor. We could study any other (p, q) -tensor (with $p + q = 2k$) obtained by raising or lowering indices in the fully-contravariant k -body Green's function. Working on fully contravariant tensors, however, will be convenient due to their higher degree of symmetry.

Let us also emphasise the simplicity of the definition of a fully contravariant k -body Green's function. Depending on the Nambu indices contained in the global μ indices, we can recover from this expression the normal as well as

any other possible anomalous components of the Green's function. In particular, for the one-body Green's function, one anomalous term appears [4]. This motivates the definition of a 2×2 matrix propagator, encompassing both normal and anomalous terms. In a way, Eq. (45) is the fully contravariant tensor generalisation of the more traditional one-body matrix Green's function. We discuss this connection in more detail in Sec. IV A, where we explicitly relate our approach to the standard Gorkov formulation exposed in Ref. [5].

Using the fact that Ω_1 contains only terms with an even number of Nambu fields, the contravariant k -body Green's function can be re-expressed as

$$(-1)^k \mathcal{G}^{\mu_1 \dots \mu_{2k}}(\tau_1, \dots, \tau_{2k}) = \frac{\left\langle \text{T} \left[e^{-\int_0^\beta ds \Omega_1(s)} A^{\mu_1}(\tau_1) \dots A^{\mu_{2k}}(\tau_{2k}) \right] \right\rangle_0}{\left\langle \text{T} e^{-\int_0^\beta ds \Omega_1(s)} \right\rangle_0}. \quad (46)$$

The (imaginary) time dependence is now with respect to Ω_0 . Expanding the exponential and permuting sums and integrals with the ensemble average, we find the perturbative expansion of the contravariant k -body Green's function:

$$(-1)^k \mathcal{G}^{\mu_1 \dots \mu_{2k}}(\tau_1, \dots, \tau_{2k}) = \sum_{n=0}^{+\infty} \frac{(-1)^n}{n!} \int_0^\beta ds_1 \dots \int_0^\beta ds_n \frac{\left\langle \text{T} [\Omega_1(s_1) \dots \Omega_1(s_n) A^{\mu_1}(\tau_1) \dots A^{\mu_{2k}}(\tau_{2k})] \right\rangle_0}{\left\langle \text{T} e^{-\int_0^\beta ds \Omega_1(s)} \right\rangle_0}. \quad (47)$$

This expression is analogous to the perturbative expansion in the normal, symmetry-conserving case [59], but replacing creation and annihilation operators by (contravariant) Nambu fields.

The integral at a given order in the perturbative expansion of the contravariant k -body Green's function can be computed as usual via a statistical time-dependent Wick's theorem. The proof of Wick's theorem can be adapted straightforwardly to the case of Nambu fields. One can follow the steps put forward in Ref. [60] and further extended to the non-Hermitian case in Ref. [57]. There are only two requirements in this derivation. First, one exploits the cyclic property of the trace. Second, the unperturbed Hamiltonian Ω_0 must be quadratic in the Nambu fields. Following these steps, the statistical time-dependent Wick's theorem reads

$$\langle A^{\mu_1}(\tau_1) \dots A^{\mu_{2p}}(\tau_{2p}) \rangle_0 = \sum_{\mathcal{P}=\{\{i,j\}\}} \epsilon(\mathcal{P}) \prod_{\substack{\{i,j\} \in \mathcal{P} \\ i < j}} \langle A^{\mu_i}(\tau_i) A^{\mu_j}(\tau_j) \rangle_0, \quad (48)$$

where the sum is over the set of pairings \mathcal{P} of the first $2p$ positive integers and $\epsilon(\mathcal{P})$ is the standard sign factor

⁴ Throughout this work we assume natural units where $\hbar = c = k_B = 1$.

associated to a pairing, \mathcal{P} . The different time-orderings in Eq. (47) are taken into account by using the unperturbed time-ordered contravariant propagator

$$-\mathcal{G}^{(0)\mu\nu}(\tau, \tau') \equiv \langle T [A^\mu(\tau)A^\nu(\tau')] \rangle_0 \quad (49)$$

and by cancelling out any double-counting in the time integration with an appropriate symmetry factor. Consequently, the contravariant k -body Green's function is decomposed into a sum of amplitudes indexed over the set of *un-oriented Feynman diagrams*. We note that the appearance of un-oriented lines in the Feynman diagrams is a consequence of using the fully contravariant propagator in Eq. (49). We now provide the resulting Feynman rules in the time and in the energy representations. For more details on the exact properties of the contravariant k -body Green's functions, we refer the reader to Part II of this work.

B. Feynman rules in the time representation

Before expressing Feynman rules in the Nambu-covariant framework, let us define a notation for partially antisymmetrised tensor coordinates. These appear in the algebraic expression of un-oriented Feynman diagram, in particular at the level of interaction vertices $v_{\mu_1 \dots \mu_k}^{(k)}$. In general, we are interested in the totally antisymmetric part of the interaction vertices. We use the standard notation given in Eq. (31), namely,

$$v_{[\mu_1 \dots \mu_{2k}]}^{(k)} \equiv \frac{1}{(2k)!} \sum_{\sigma \in S_{2k}} \epsilon(\sigma) v_{\mu_{\sigma(1)} \dots \mu_{\sigma(2k)}}^{(k)}. \quad (50)$$

We stress that this vertex is totally antisymmetric. This is in contrast to the standard antisymmetrisation in Hugenholtz diagrammatics where vertices are antisymmetric only when swapping fermionic indices associated to creation and annihilation operators separately.

An important subtlety that arises in NCPT has to do with the interaction matrix elements in diagrams involving tadpoles. In the case of a vertex with p tadpoles, one needs to perform a sum over a subset of the permutations of the indices. We use the following notation,

$$v_{[\mu_1 \dots \dot{\mu}_x \dots \dot{\mu}_y \dots \mu_{2k}]}^{(k)} \equiv \frac{2^p p!}{(2k)!} \sum_{\sigma \in S_{2k}/S_2^p \times S_p} \epsilon(\sigma) v_{\mu_{\sigma(1)} \dots \dot{\mu}_x \dots \dot{\mu}_y \dots \mu_{\sigma(2k)}}^{(k)}, \quad (51)$$

where the sum is to be understood as running only over the permutations σ that *do not* exchange two indices within a dotted pair *nor* two different dotted pairs of indices. We denote the subset of these specific permutations as $S_{2k}/S_2^p \times S_p$.

Having established our notations, we now proceed to give the Feynman rules in the time domain. The n^{th} order contribution to $(-1)^k \mathcal{G}^{\mu_1 \dots \mu_{2k}}(\tau_1, \dots, \tau_{2k})$ is obtained as follows:

1. Draw all topologically distinct un-oriented unlabelled linked diagrams \mathcal{G}_n with n vertices and $2k$ external lines. Two diagrams are topologically equivalent if one is obtained from the other by a continuous deformation.
2. Assign a label $\tau_1 \dots \tau_n$ to the vertices and compute the symmetry factor S which is the number of permutations of vertex labels leaving invariant the labelled diagram (up to a continuous deformation).
3. Assign a global index $\mu = (b, l_b)$ to any half-line of \mathcal{G}_n . For every line joining (μ, τ) and (ν, τ') , multiply by a factor $-\mathcal{G}^{(0)\mu\nu}(\tau, \tau')$. In the case of a tadpole, the factor reads $-\mathcal{G}^{(0)\mu\nu}(\tau + \eta, \tau)$ with $\eta \rightarrow 0^+$.
4. For each k_i -body vertex with indices $\mu_1 \dots \mu_{2k_i}$, multiply by a factor $v_{[\mu_1 \dots \mu_{2k_i}]}^{(k_i)}$ where indices belonging to a same tadpole are dotted in the same way, according to Eq. (51).
5. Sum over global indices $\mu = (b, l_b)$ and integrate over τ on $[0, \beta]$.
6. Multiply by a factor $\frac{(-1)^{n+L}}{S \times 2^T \prod_{l=2}^{l_{\max}} (l!)^m}$ where L is the number of loops (including tadpoles), m the number of l -tuple equivalent lines (with $l \in \llbracket 2, l_{\max} \rrbracket$) and T the number of tadpoles.

In the above rules, we choose to work with a time conventionally flowing from the bottom to the top of the diagram. The reading convention of a line is from top to bottom while the writing of the algebraic expression is from left to right. For vertices and tadpoles, indices are to be read clockwise from the angle $+\pi$ towards $-\pi$ and the writing is still from left to right. In the case of no external legs, i.e. $k = 0$, we obtain the n^{th} order contribution to $\ln \frac{Z}{Z_0}$ rather than to a Green's function.

Just like in standard versions of perturbation theory, the linked-cluster theorem allows us to consider only linked diagrams. The resulting Feynman amplitude $\mathcal{A}^{\mu_1 \dots \mu_{2k}}(\tau_{\mu_1}, \dots, \tau_{\mu_{2k}})$ associated with the un-oriented Feynman diagram \mathcal{G}_n , which contributes to $(-1)^k \mathcal{G}^{\mu_1 \dots \mu_{2k}}(\tau_1, \dots, \tau_{2k})$, reads generically

$$\begin{aligned} \mathcal{A}^{\mu_1 \dots \mu_{2k}}(\tau_{\mu_1}, \dots, \tau_{\mu_{2k}}) &= \frac{(-1)^{n+L}}{S \times 2^T \prod_{l=2}^{l_{\max}} (l!)^m} \\ &\times \sum_{\lambda \dots \lambda} v_{[\lambda \dots \lambda]}^{(k_1)} \dots v_{[\lambda \dots \lambda]}^{(k_n)} \int_0^\beta d\tau_1 \dots d\tau_n \prod_{e \in I} -\mathcal{G}^{(0)\lambda\lambda}(\tau_i, \tau_j) \\ &\times \prod_{e \in E_{\text{in}}} -\mathcal{G}^{(0)\lambda\mu}(\tau_i, \tau_\mu) \prod_{e \in E_{\text{out}}} -\mathcal{G}^{(0)\mu\lambda}(\tau_\mu, \tau_j), \quad (52) \end{aligned}$$

where λ and μ denote respectively generic global indices for internal and (incoming or outgoing) external lines⁵.

⁵ Diagrams are un-oriented here, so “outgoing” or “incoming” lines are to be understood with respect to the time flow.

Labels k_i characterise the k -body type of vertex i and τ_i denotes the corresponding imaginary-time label. The set of internal, incoming external and outgoing external lines are respectively denoted by I , E_{in} and E_{out} . In Eq. (52) the tadpole case is not explicitly taken into account for the sake of conciseness.

Let us make the following observations about the Feynman rules above. In the case where the vertex is free of tadpoles, only its totally antisymmetric part contributes to the Feynman amplitude. This generalises what was noticed by De Dominicis and Martin [13, 14], Kleiner [15, 16] and Haussmann [17, 18] to the case of a generic k -body interaction and a general extended basis. In the case where the vertex is contracted with a set of tadpoles, it is actually a specific partial antisymmetrisation that contributes to the Feynman amplitude. Let us point out that this subtle case of partial antisymmetrisation is neither mentioned in Refs. [13–18] nor, to our knowledge, elsewhere. The occurrence of totally and partially antisymmetric vertices is the consequence of a factorisation of several Feynman diagrams. This factorisation property, in turn, arises because the Feynman amplitudes are expressed in terms of:

- A sum over pairings, thanks to Wick's theorem (48);
- A sum over single-particle and Nambu indices, thanks to our decomposition of Ω_0 and Ω_1 as polynomials in Nambu fields in Eqs. (43);
- Fully covariant vertices, which can be antisymmetrised while keeping their tensor character intact.

More details on how totally and partially antisymmetric vertices arise in the above Feynman rules are given in App. B. The factorisation property is discussed in connection with standard Gorkov and Bogoliubov formalisms in Sec. IV.

We stress again that the NCPT requires an *extension the Hugenholtz antisymmetrisation of vertices*. In standard Hugenholtz diagrammatics, vertices are only antisymmetric with respect to permutations of outgoing and incoming half-lines, separately. Here, in contrast, the antisymmetrisation is complete. This antisymmetrisation is closely related to the *ad hoc* factorisation that was seen to appear in the zero-temperature Gorkov formalism of Ref. [5]. There, several oriented Feynman diagrams contributing to the self-energy at second order were factorised to get a simpler expression in Eqs. (79) of [5]. This factorization required the introduction of the so-called \mathcal{C} and \mathcal{D} objects, defined in Eqs. (78) of Ref. [5]. The NCPT developed here shows why such factorisation is no coincidence. Moreover, our approach generalises these considerations to any set of Feynman diagrams, and to the non-zero temperature case.

Finally, we stress that the amplitude associated to an un-oriented Feynman diagram, Eq. (52), is essentially a tensor network of covariant vertices and contravariant propagators. As a consequence, the amplitude associated to an un-oriented Feynman diagram is a tensor of the

same nature as the k -body Green's function to which it contributes.

C. Feynman rules in the energy representation

Similarly to other formalisms of perturbation theory, the time-independence of the partitioning in Eq. (43) allows us to simplify the Feynman amplitudes when working in the energy representation. Before stating the Feynman rules in the energy representation, however, we need to specify the conventions we are using to define the propagators in their energy representation. In thermal equilibrium, the unperturbed contravariant one-body propagator only depends on the time difference, i.e.

$$\mathcal{G}^{(0)\mu\nu}(\tau + \tau', \tau') = \mathcal{G}^{(0)\mu\nu}(\tau, 0) \equiv \mathcal{G}^{(0)\mu\nu}(\tau). \quad (53)$$

Furthermore, the propagator is a β -quasiperiodic function, i.e.

$$\mathcal{G}^{(0)\mu\nu}(\tau + \beta) = -\mathcal{G}^{(0)\nu\mu}(\tau), \quad (54)$$

and fulfils the antisymmetry property

$$\mathcal{G}^{(0)\mu\nu}(\tau) = -\mathcal{G}^{(0)\nu\mu}(-\tau). \quad (55)$$

As a consequence, the Fourier transform of the unperturbed contravariant propagator yields the energy representation

$$\mathcal{G}^{(0)\mu\nu}(\omega_m) \equiv \int_0^\beta d\tau e^{i\omega_m\tau} \mathcal{G}^{(0)\mu\nu}(\tau), \quad (56)$$

$$\mathcal{G}^{(0)\mu\nu}(\tau) = \frac{1}{\beta} \sum_m e^{-i\omega_m\tau} \mathcal{G}^{(0)\mu\nu}(\omega_m), \quad (57)$$

where $\omega_m \equiv (2m + 1)\frac{\pi}{\beta}$ are fermionic Matsubara frequencies.

These considerations are easily extended to k -body propagators. Energy conservation dictates that contravariant k -body Green's functions are Fourier transformed to their energy representation leaving out a factor $\beta\delta_{\omega_{\text{in}},\omega_{\text{out}}}$,

$$\begin{aligned} & \mathcal{G}^{\mu_1 \dots \mu_{2k}}(\omega_{m_1}, \dots, \omega_{m_{2k}}) \beta\delta_{\omega_{\text{in}},\omega_{\text{out}}} \\ & \equiv \int_0^\beta d\tau_1 \dots d\tau_{2k} e^{+i\omega_{m_{\text{in}}}\tau_{m_{\text{in}}} + \dots} e^{-i\omega_{m_{\text{out}}}\tau_{m_{\text{out}}} - \dots} \\ & \quad \times \mathcal{G}^{\mu_1 \dots \mu_{2k}}(\tau_1, \dots, \tau_{2k}), \end{aligned} \quad (58)$$

$$\begin{aligned} & \mathcal{G}^{\mu_1 \dots \mu_{2k}}(\tau_1, \dots, \tau_{2k}) \\ & = \frac{1}{\beta^{2k}} \sum_{\omega_{m_1} \dots \omega_{m_{2k}}} e^{-i\omega_{m_{\text{in}}}\tau_{m_{\text{in}}} - \dots} e^{+i\omega_{m_{\text{out}}}\tau_{m_{\text{out}}} + \dots} \\ & \quad \times \mathcal{G}^{\mu_1 \dots \mu_{2k}}(\omega_{m_1}, \dots, \omega_{m_{2k}}) \beta\delta_{\omega_{\text{in}},\omega_{\text{out}}}. \end{aligned} \quad (59)$$

Here, ω_{in} and ω_{out} denote respectively the sum of the external incoming and outgoing energies of the Green's

function⁶. Energies flowing in and out are denoted generically as $\omega_{m_{\text{in}}}$ and $\omega_{m_{\text{out}}}$, respectively. Their associated times are also generically denoted as $\tau_{m_{\text{in}}}$ and $\tau_{m_{\text{out}}}$, respectively.

With the above definitions for the energy representation of contravariant many-body Green's functions, the n^{th} order contribution to $(-1)^k \mathcal{G}^{\mu_1 \dots \mu_{2k}}(\omega_{m_1}, \dots, \omega_{m_{2k}})$ is obtained as follows:

1. Draw all topologically distinct un-oriented unlabelled linked diagrams \mathcal{G}_n with n vertices and $2k$ external lines. Two diagrams are topologically equivalent if one is obtained from the other by a continuous deformation.
2. Assign a label $1 \dots n$ to the vertices and compute the symmetry factor S which is the number of permutations of vertex labels leaving invariant the labelled diagram (up to a continuous deformation).
3. Choose a spanning forest of \mathcal{G}_n ⁷. For each internal line l_i not in the forest, assign an independent Matsubara frequency ω_{l_i} . Remaining internal lines are assigned the linear combination of ω_{l_i} and external ω_{m_j} determined by conservation of energy at each vertex. The Matsubara frequency thus associated to any line e is denoted generically as ω_e .
4. Assign a global index $\mu = (b, l_b)$ to any half-line of \mathcal{G}_n . For each line e , joining half-lines μ to ν , multiply by a factor $-\mathcal{G}^{(0)\mu\nu}(\omega_e)$. In the case of a tadpole, the factor reads $-\mathcal{G}^{(0)\mu\nu}(\omega_e)e^{-i\omega_e\eta}$ with $\eta \rightarrow 0^+$.
5. For each k_i -body vertex with indices $\mu_1 \dots \mu_{2k_i}$ multiply by a factor $v_{[\mu_1 \dots \mu_{2k_i}]}$ where indices belonging to a same tadpole are dotted in the same way, according to Eq. (51).
6. Sum over global indices $\mu = (b, l_b)$ as \sum_{μ} and over the L independent Matsubara frequencies ω_{l_i} (defined for the chosen spanning forest) as $\frac{1}{\beta} \sum_{\omega_{l_i}}$. By definition L is the total number of loops, including tadpoles.
7. Multiply by a factor $\frac{(-1)^{n+L} \beta^{C-1}}{S \times 2^T \prod_{l=2}^{l_{\text{max}}} (l!)^m}$ where C is the number of connected components, m the number of l -tuple equivalent lines (with $l \in \llbracket 2, l_{\text{max}} \rrbracket$) and T the number of tadpoles.

In the above rules, the energy flow convention is left to be specified. We discuss this choice further in Sec. III D,

where Matsubara sums are performed explicitly. The reading convention of a line is going against the energy flow orientation while the writing of the associated propagator is from left to right. The reading of vertices is the same as for the Feynman rules in the time representation. The factor β^C appears from the change of representation from time to energy [58], and the remaining β^{-1} from our choice to factorise the global term $\beta \delta_{\omega_{\text{in}}, \omega_{\text{out}}}$ out of the definition of the energy representation of the k -body Green's function. In the case of $k = 0$, we obtain the n^{th} order contribution to $\frac{1}{\beta} \ln \frac{Z}{Z_0}$ rather than to a Green's function.

Following the above diagrammatic rules, the resulting Feynman amplitude $\mathcal{A}^{\mu_1 \dots \mu_{2k}}(\omega_{m_1}, \dots, \omega_{m_{2k}})$ associated to the un-oriented Feynman diagram \mathcal{G}_n reads generically

$$\begin{aligned} \mathcal{A}^{\mu_1 \dots \mu_{2k}}(\omega_{m_1}, \dots, \omega_{m_{2k}}) &= \frac{(-1)^{n+L} \beta^{C-1}}{S \times 2^T \prod_{l=2}^{l_{\text{max}}} (l!)^m} \\ &\times \sum_{\lambda \dots \lambda} v_{[\lambda \dots \lambda]}^{(k_1)} \dots v_{[\lambda \dots \lambda]}^{(k_n)} \frac{1}{\beta^L} \sum_{\omega_{l_1} \dots \omega_{l_L}} \prod_{e \in I} -\mathcal{G}^{(0)\lambda\lambda}(\omega_e) \\ &\times \prod_{e \in E_{\text{in}}} -\mathcal{G}^{(0)\lambda\mu}(\omega_{m_{\text{in}}}) \prod_{e \in E_{\text{out}}} -\mathcal{G}^{(0)\mu\lambda}(\omega_{m_{\text{out}}}), \quad (60) \end{aligned}$$

where λ and μ denote respectively generic global indices for internal and (incoming or outgoing) external lines⁸. For each vertex i , the label k_i indicates that this is a k_i -body interaction. Independent Matsubara frequencies that are summed over are denoted by ω_{l_i} . External incoming and outgoing Matsubara frequencies are generically denoted as $\omega_{m_{\text{in}}}$ and $\omega_{m_{\text{out}}}$, respectively. Internal Matsubara frequencies, which are linear combinations of ω_{l_i} , $\omega_{m_{\text{in}}}$ and $\omega_{m_{\text{out}}}$, are generically denoted as ω_e . Again, I denotes the set of internal lines, E_{in} the set of incoming external lines and E_{out} the set of outgoing external lines. In Eq. (60) the tadpole case is not explicitly taken into account for the sake of conciseness.

Let us stress that it is not the first time that un-oriented diagrams occur in formal many-body theory work. Those do appear sometimes in classical textbooks, such as Ref. [58]. However, to the best of our knowledge un-oriented diagrams have always been either restricted to Majorana fields, or were to be understood as a shorthand notation for summing over amplitudes associated to all compatible oriented diagrams, such as in Ref. [61]. Such shorthand notation appears already in the work of Nambu on superconductivity [11], for instance. Making the distinction between this common shorthand notation and the NCPT diagrammatics obtained here is essential. In the former approach, e.g. see the diagrammatic rules given in Chap. 7 of [61], the dependence on Nambu indices of the Feynman amplitude arises from two different sources. On the one hand, the amplitude is the result of a sum of

⁶ The external energy flow is left to be fixed by convention.

⁷ By definition, a spanning forest of the diagram \mathcal{G}_n is a sub-diagram without cycles which is maximal in the sense that no line can be added to the sub-diagram without creating a cycle. It necessarily contains all the vertices of \mathcal{G}_n .

⁸ Diagrams are un-oriented here, so ‘‘outgoing’’ or ‘‘incoming’’ lines are to be understood with respect to the energy flow.

several single-particle tensor networks whose values depend on the kind of propagators at stake, i.e. on Nambu indices. On the other hand, there is an additional effect on the symmetry factor of the amplitude. For example, in Ref. [61], a factor $\frac{1}{2}$ arises for each anomalous tadpole, but not for normal tadpoles. The factor due to equivalent lines also typically depends on Nambu indices. Such non-trivial dependence on the Nambu indices obscures the study of Nambu-covariance of the amplitudes contributing to the many-body Green's functions, and precludes transparent formal and numerical developments.

In contrast, in the Feynman rules of NCPT, given in Secs. III B and III C, the symmetry factor arises solely from the topology of the un-oriented diagram. There is no explicit dependence of the symmetry factor on Nambu indices. With these rules, the amplitude of an un-oriented diagram is thus clearly decoupled into a Nambu tensor network, and a symmetry (and sign) factor. To the best of our knowledge, the only occurrence of similar un-oriented diagrammatic rules is in the work by De Dominicis and Martin [13, 14], Kleinert [15] and Haussmann [17]. We emphasise, however, that these derivations were performed with restrictive hypotheses on the choice of extended basis and Hamiltonian, and that the connection with the concept of Nambu tensors and covariance appears to have remained unnoticed.

D. Gaudin's summation rules

Feynman amplitudes, as obtained by applying the rules of the previous subsection, provide a decomposition of Green's functions in terms of tensor networks *and* of sums over Matsubara frequencies, as explicitly shown in Eq. (60). The sums over Matsubara frequencies can be performed exactly by considering all different orderings of vertices of a given diagram. Such decomposition gives up to $n!$ terms, with n the number of vertices of the diagram. An alternative method is based on applying the residue theorem until all Matsubara sums have been replaced by complex integrals.

A third, more convenient approach to tackle the Matsubara sums consists in decomposing a given Feynman amplitude into a sum of contributions, one for each spanning forest of a diagram, as shown by Gaudin in Ref. [62]. Compared to the residue theorem, only diagrammatic considerations are necessary. Compared to vertex ordering, the number of spanning forests grows much more slowly with n . For example, the number of spanning forests for a connected diagram with only two-body vertices is bounded from above by $4^{n-1} \ll n!$. In Ref. [62], Gaudin derived a set of diagrammatic rules giving the algebraic expression of a Feynman diagram which is obtained after performing sums over Matsubara frequencies. His focus was on two-particle-irreducible (2PI) diagrams with dressed propagators at finite β in a symmetry-conserving case. This approach has been exploited several times in a very similar fashion for different applications [63–66].

As noted in Ref. [67], Gaudin's work on the summation rules remains relatively unknown, so we recapitulate the general rationale behind these rules and adapt them to the diagrams of NCPT in the energy representation. For simplicity, we focus on connected diagrams without tadpoles nor external lines. In this case, all spanning forests are connected, i.e. they are (by definition) spanning trees. The extension to the case of a general diagram is detailed in App. C.

1. Rationale

In general, a contravariant propagator can be expressed in terms of a spectral function $S^{\mu\nu}(\epsilon)$,

$$\mathcal{G}^{\mu\nu}(\omega_m) = \int_{-\infty}^{+\infty} \frac{d\epsilon}{2\pi} \frac{S^{\mu\nu}(\epsilon)}{i\omega_m - \epsilon}. \quad (61)$$

This so-called spectral representation of a propagator is discussed, along with other exact properties, in Part II of this work. We are interested in the unperturbed contravariant propagator $\mathcal{G}^{(0)\mu\nu}(\omega_m)$, associated to a Hamiltonian Ω_0 which is quadratic in the Nambu fields. In this case, the spectral function associated to $\mathcal{G}^{(0)\mu\nu}(\omega_m)$ is expressed as

$$S^{(0)\mu\nu}(\epsilon) = \sum_n X^{(n)\mu} \bar{X}^{(n)\nu} (2\pi) \delta(\epsilon - \epsilon_n), \quad (62)$$

where ϵ_n are quasiparticle energies and $X^{(n)\mu}$, the associated spectroscopic amplitudes. By definition, ϵ_n are the eigenvalues of the matrix made of the mixed $(1, 1)$ coordinates $U^\mu{}_\nu$. We assume these eigenvalues are labelled by the discrete quantum number n (not to be confused with the order in perturbation theory) and are non-degenerate, for simplicity. $X^{(n)\mu}$ and $\bar{X}_\mu^{(n)}$ are, respectively, the coordinates of the associated right and left eigenvectors,

$$\sum_\nu U^\mu{}_\nu X^{(n)\nu} = \epsilon_n X^{(n)\mu}, \quad (63a)$$

$$\sum_\nu \bar{X}_\mu^{(n)} U^\mu{}_\nu = \epsilon_n \bar{X}_\nu^{(n)}. \quad (63b)$$

These eigenvectors are normalised such that they form a biorthogonal system, i.e.

$$\sum_\mu \bar{X}_\mu^{(n)} X^{(n')\mu} = \delta_{nn'}. \quad (64)$$

Note that the antisymmetry of $U_{\mu\nu}$ would in principle provide a relation between the left and right eigenvectors. For clarity, however, we keep a notation that distinguishes them explicitly.

The rationale behind Gaudin's summation rules is the following. Let \mathcal{G}_n be a connected un-oriented Feynman diagram with L loops and no tadpoles nor external lines.

The problem is to compute within Eq. (60) the following sum

$$I(\mathcal{G}_n) \equiv \frac{1}{\beta^L} \sum_{\omega_{l_1} \dots \omega_{l_L}} \prod_{e \in I} -\mathcal{G}^{(0)\lambda\lambda}(\omega_e). \quad (65)$$

Replacing each propagator by the corresponding spectral representation in Eq. (61), Eq. (65) reads

$$I(\mathcal{G}_n) = \int_{-\infty}^{+\infty} \left(\prod_{e \in I} S^{(0)\lambda\lambda}(\epsilon_e) d\epsilon_e \right) \times \frac{1}{\beta^L} \sum_{\omega_{l_1} \dots \omega_{l_L}} \left(\prod_{e \in I} \frac{1}{\epsilon_e - i\omega_e} \right), \quad (66)$$

where ϵ_e denotes the energy associated to the line e . The problem is thus reduced to computing

$$\frac{1}{\beta^L} \sum_{\omega_{l_1} \dots \omega_{l_L}} \left(\prod_{e \in I} \frac{1}{\epsilon_e - i\omega_e} \right), \quad (67)$$

where each ω_e is a linear combination of L independent Matsubara frequencies ω_{l_i} , obtained by applying energy conservation laws at the vertices of \mathcal{G}_n . To compute it, the above product is decomposed into partial fractions, where each term is associated to one spanning tree \mathcal{A} of \mathcal{G}_n . The Matsubara sums in each spanning tree term are decoupled and performed analytically. As a result, $I(\mathcal{G}_n)$ is decomposed as

$$I(\mathcal{G}_n) = \sum_{\mathcal{A} \in \text{Spanning trees}} I(\mathcal{A}). \quad (68)$$

In the case of a dressed propagator, the resulting expression for $I(\mathcal{G}_n)$ contains energy integrals of a product of spectral functions multiplied by the factor in Eq. (67). In the case of an unperturbed one-body propagator with a spectral function given by Eq. (62), the energy integrals simplify to sums over quasiparticle energies and the spectral functions $S^{\mu\nu}(\epsilon_e)$ are replaced by the spectroscopic amplitudes $X^{(n_e)\mu} \bar{X}^{(n_e)\nu}$. The factor (67) remains the same in both cases. Eventually, $I(\mathcal{G}_n)$ is plugged back into Eq. (60), which reads generically

$$\begin{aligned} \mathcal{A}^{\mu_1 \dots \mu_{2k}}(\omega_{m_1}, \dots, \omega_{m_{2k}}) = \\ \frac{(-1)^{n+L} \beta^{C-1}}{S \times 2^T \prod_{l=2}^{l_{\max}} (l!)^m} \sum_{\lambda \dots \lambda} v_{[\lambda \dots \lambda]}^{(k_1)} \dots v_{[\lambda \dots \lambda]}^{(k_n)} \times I(\mathcal{G}_n). \end{aligned} \quad (69)$$

The sum of Matsubara sums, $I(\mathcal{G}_n)$, can be evaluated explicitly by following a set of summation rules that we enumerate below.

2. Summation rules

We start by defining the complementary diagram, \mathcal{B} , of a given spanning tree \mathcal{A} in a diagram \mathcal{G}_n . The complementary diagram \mathcal{B} is the diagram made of all the vertices

of \mathcal{G}_n and of all the lines of \mathcal{G}_n that are not present in the set of lines of \mathcal{A} . Further, we denote the lines belonging to \mathcal{A} as a, b, \dots , lines belonging to \mathcal{B} as p, q, \dots , and a generic line of \mathcal{G}_n by e . In the following, ϵ_{n_e} indicates the quasiparticle energy associated to a fermion line e . The function $f(\epsilon)$ is the standard Fermi-Dirac distribution, i.e. $f(\epsilon) \equiv \frac{1}{1+e^{\beta\epsilon}}$.

Let \mathcal{G}_n be a connected diagram of order n without tadpoles nor external lines. The Matsubara sum $I(\mathcal{G}_n)$ is obtained in terms of the spectroscopic amplitudes, $X^{(n_e)\mu}$ and $\bar{X}^{(n_e)\nu}$, and quasiparticle energies, ϵ_{n_e} , as follows:

1. Build the set of spanning trees \mathcal{A} of \mathcal{G}_n . Associate a complementary diagram \mathcal{B} to each spanning tree.
2. Fix an orientation on the diagram, i.e. associate a choice of direction and an intensity integer n_e to each line such that for each cycle (p) , associated to the line p of \mathcal{B} ⁹, its total orientation N_p is different from 0. The total orientation N_p of a cycle (p) is obtained by adding n_e for each line e of the cycle oriented in the same way as p , and by subtracting n_e for each line e of the cycle oriented in the opposite way to p .
3. The Matsubara sum $I(\mathcal{G}_n)$ is the sum of the contributions $I(\mathcal{A})$ associated to each spanning tree \mathcal{A} . $I(\mathcal{A})$ is the sum over quasiparticle energies ϵ_{n_e} of a product of statistical factors, one for each line p in \mathcal{B} ; of energy denominators, one for each line a in \mathcal{A} ; and of spectroscopic amplitudes, one for each line e in \mathcal{G}_n . The contribution of one spanning tree $I(\mathcal{A})$ is obtained as follows:
 - 3.a. For each line p in \mathcal{B} , multiply by the statistical factor $f(-\epsilon_{n_p})$ or $-f(\epsilon_{n_p})$, depending on whether N_p is positive or negative, respectively.
 - 3.b. For each line a in \mathcal{A} , multiply by the energy denominator obtained as follows: when removing the line a from \mathcal{A} the tree is divided in two sub-trees \mathcal{A}^+ and \mathcal{A}^- defined such that a is oriented from \mathcal{A}^- towards \mathcal{A}^+ . The denominator is the sum of ϵ_{n_e} for each line connecting \mathcal{A}^- to \mathcal{A}^+ , positively or negatively counted when going in the same or opposite direction as a , respectively. Note that by definition the denominator contains a $+\epsilon_{n_a}$ term.
 - 3.c. For each line e in \mathcal{G}_n multiply by a factor $X^{(n_e)\mu_e} \bar{X}^{(n_e)\nu_e}$ and sum over n_e which indexes the quasiparticle energies and spectroscopic amplitudes associated to the line e .

Reading and writing conventions are the same as in Sec. III C given the orientation fixed in the summation

⁹ For each spanning tree \mathcal{A} and line p in \mathcal{B} , the cycle (p) is uniquely defined as the one obtained when adding p to \mathcal{A} .

rule 2 (without taking into account the chosen intensities). Examples of application of the above rules are given in Sec. III E. Following Gaudin's summation rules, the Feynman amplitude associated to \mathcal{G}_n reads

$$\begin{aligned} \mathcal{A}^{\mu_1 \dots \mu_{2k}}(\omega_{m_1}, \dots, \omega_{m_{2k}}) &= \frac{(-1)^{n+L} \beta^{C-1}}{S \times 2^T \prod_{l=2}^{l_{\max}} (l!)^m} \\ &\times \sum_{\lambda \dots \lambda} v_{[\lambda \dots \lambda]}^{(k_1)} \dots v_{[\lambda \dots \lambda]}^{(k_n)} \\ &\times \sum_{n_e \dots n_e} \prod_{e \in I} X^{(n_e)\lambda} \bar{X}^{(n_e)\lambda} \sum_{\mathcal{A}} \frac{N(\mathcal{B})}{D(\mathcal{A})}, \quad (70) \end{aligned}$$

where n_e denotes a generic index for quasiparticle energies and spectroscopic amplitudes associated to a line e . The notation \mathcal{A} denotes a generic spanning tree, \mathcal{B} its complementary diagram, $N(\mathcal{B})$ the numerator obtained following summation rule 3.a. and $D(\mathcal{A})$ the denominator obtained following summation rule 3.b. Although not displayed in Eq. (70), we stress that $N(\mathcal{B})$ and $D(\mathcal{A})$ depend on the quasiparticle energies ϵ_{n_e} .

3. Discussion

The summation rules just discussed decompose $I(\mathcal{G}_n)$ into a sum of contributions $I(\mathcal{A})$, one for each spanning tree as in Eq. (68). When looking at the contribution for one spanning tree \mathcal{A} , several infrared divergences might appear, i.e. divergences due to a denominator (computed in rule 3.b.) converging to zero. The problem is even worse in the case of a translation invariant system where some denominators are *only* evaluated when they are vanishing because of momentum conservation at vertices and of the unperturbed propagator being diagonal in momentum. This was originally the reason why only 2PI diagrams were considered in Ref. [62]. Since then, the origin of these divergences has been pinpointed to stem from the splitting of $I(\mathcal{G}_n)$ into spanning tree contributions, Eq. (68). When the set of spanning tree contributions are added up, the infrared divergences cancel out. This cancellation of infrared divergences is briefly discussed in App. B of Ref. [67] and in Chaps. 2-3 of Ref. [68]. It was shown there that the infrared divergences appearing in Gaudin's formulae are artificial, and always cancel out when combining several spanning tree contributions.

Typically, the limit where a denominator, made of a linear combination of quasiparticle energies, goes to zero is cancelled out by the combination of several numerators (from different spanning trees) going also to zero - so that the overall ratio converges to a well-defined finite value. In practical implementations, numerical instabilities can be avoided by replacing the ratio by a Taylor expansion of the numerator simplified by the denominator. In doing this, derivatives of the statistical distributions appear. We study one of these examples in Sec. III E: a diagram at third order which is not 2PI. It is explicitly shown there how spanning tree contributions get their infrared diver-

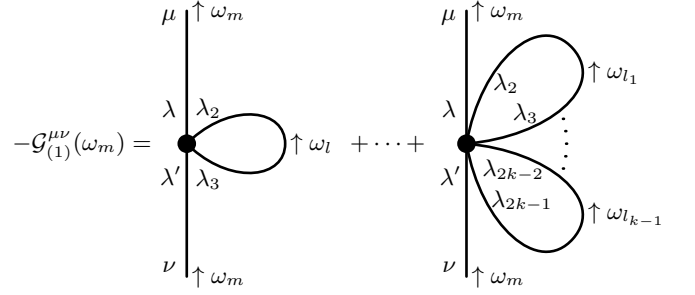


FIG. 1. Labeled diagrams contributing to the propagator at first order with 2- up to k -body interactions. The orientation convention for the energy flow is also made explicit.

gences cancelled out. We also give an asymptotically valid expression around a removable singularity depending on the derivative of the Fermi-Dirac distribution. Obtaining explicit rules which systematically remove those artificial infrared divergences would be interesting to automatically and efficiently generate expressions free of potential numerical instabilities. Such refinements are beyond the scope of this article.

E. Examples

In this section, we give some basic and illustrative applications of the Feynman rules of NCPT. Contributions at first, second and third order of the contravariant one-body Green's function are worked out explicitly. The factorisation of energy denominators and the cancellation of infrared divergences is then briefly discussed.

1. First order perturbations

As a first example, we consider the system and partitioning defined by

$$\begin{aligned} \Omega_0 &\equiv \frac{1}{2} \sum_{\mu\nu} U_{\mu\nu} A^\mu A^\nu, \\ \Omega_1 &\equiv \sum_{k=2}^{k_{\max}} \frac{1}{(2k)!} \sum_{\mu_1 \dots \mu_{2k}} v_{\mu_1 \dots \mu_{2k}}^{(k)} A^{\mu_1} \dots A^{\mu_{2k}}. \end{aligned}$$

At first order in terms of number of vertices, the set of diagrams contributing is shown in Fig. 1. If $k_{\max} = 2$, the Feynman amplitude $-\mathcal{A}_{(1)}^{\mu\nu}(\omega_m)$ contributing to $\mathcal{G}_{(1)}^{\mu\nu}(\omega_m)$ reads

$$\begin{aligned} -\mathcal{A}_{(1)}^{\mu\nu}(\omega_m) &= \sum_{\lambda\lambda'} \mathcal{G}^{(0)\mu\lambda}(\omega_m) \\ &\times \left[\frac{1}{2} \sum_{\lambda_2\lambda_3} v_{[\lambda\lambda_2\lambda_3\lambda']}^{(2)} \frac{1}{\beta} \sum_{\omega_l} \mathcal{G}^{(0)\lambda_2\lambda_3}(\omega_l) e^{-i\omega_l\eta} \right] \\ &\times \mathcal{G}^{(0)\lambda'\nu}(\omega_m). \quad (71) \end{aligned}$$

Using Eq. (C1), the Matsubara sum associated to the tadpole can be performed and Eq. (71) becomes

$$\begin{aligned}
-\mathcal{A}_{(1)}^{\mu\nu}(\omega_m) &= \sum_{\lambda\lambda'} \mathcal{G}^{(0)\mu\lambda}(\omega_m) \\
&\times \left[\frac{1}{2} \sum_{\lambda_2\lambda_3} v_{[\lambda\lambda_2\lambda_3\lambda']}^{(2)} \right. \\
&\quad \left. \times \sum_{n_t} f(-\epsilon_{n_t}) X^{(n_t)\lambda_2} \bar{X}^{(n_t)\lambda_3} \right] \\
&\times \mathcal{G}^{(0)\lambda'\nu}(\omega_m), \tag{72}
\end{aligned}$$

where n_t indexes quasiparticle energies and their associated spectroscopic amplitudes.

For a general k_{\max} -body interaction, the same first-order contribution reads

$$\begin{aligned}
-\mathcal{A}_{(1)}^{\mu\nu}(\omega_m) &= \\
&\sum_{\lambda\lambda'} \mathcal{G}^{(0)\mu\lambda}(\omega_m) \left\{ \sum_{k=2}^{k_{\max}} \left[\frac{1}{2^{k-1}(k-1)!} \sum_{\lambda_2\dots\lambda_{2k-1}} v_{[\lambda\lambda_2\lambda_3\lambda_4\lambda_5\dots\lambda']}^{(k)} \right. \right. \\
&\quad \left. \left. \times \prod_{j=1}^{k-1} \left(\frac{1}{\beta} \sum_{\omega_{l_j}} \mathcal{G}^{(0)\lambda_{2j}\lambda_{2j+1}}(\omega_{l_j}) e^{-i\omega_{l_j}\eta_j} \right) \right] \right\} \times \mathcal{G}^{(0)\lambda'\nu}(\omega_m). \tag{73}
\end{aligned}$$

In Eq. (73), the $k-1$ different tadpoles are denoted with indices dotted a different number of times. Just like for Eq. (72), Matsubara sums can be explicitly performed so that $-\mathcal{A}_{(1)}^{\mu\nu}(\omega_m)$ reads

$$\begin{aligned}
-\mathcal{A}_{(1)}^{\mu\nu}(\omega_m) &= \\
&\sum_{\lambda\lambda'} \mathcal{G}^{(0)\mu\lambda}(\omega_m) \left\{ \sum_{k=2}^{k_{\max}} \left[\frac{1}{2^{k-1}(k-1)!} \sum_{\lambda_2\dots\lambda_{2k-1}} v_{[\lambda\lambda_2\lambda_3\lambda_4\lambda_5\dots\lambda']}^{(k)} \right. \right. \\
&\quad \left. \left. \times \prod_{j=1}^{k-1} \left(\sum_{n_j} f(-\epsilon_{n_j}) X^{(n_j)\lambda_{2j}} \bar{X}^{(n_j)\lambda_{2j+1}} \right) \right] \right\} \mathcal{G}^{(0)\lambda'\nu}(\omega_m), \tag{74}
\end{aligned}$$

where n_j indexes the j^{th} tadpole quasiparticle energies and associated spectroscopic amplitudes.

Eqs. (71) and (73), when stripped off the contraction with external propagators, are closely related to the self-consistent HFB self-energies with up to k_{\max} -body interactions. If Eq. (71) is only slightly more simple than the HFB equation with a two-body interaction, Eq. (73) is remarkably simple and compact compared to what one would expect from the HFB equations with arbitrary large k -body interactions. Note, in particular, that different contractions with normal and anomalous lines would have to be considered explicitly. Importantly, the more complex the interaction is (the higher the k), the more powerful is the simplification coming from NCPT. We discuss the HFB equations in more detail in Part II, together with other self-consistent many-body approximations.

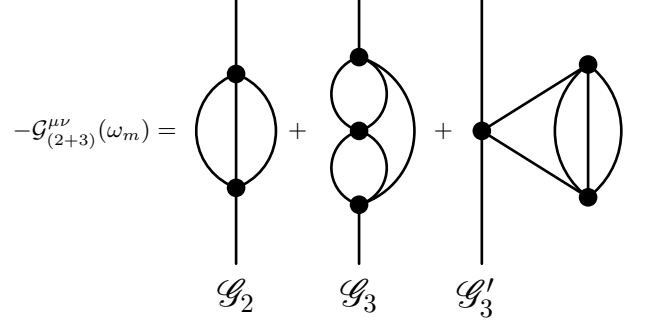


FIG. 2. Diagrams contributing to the one-body Green's function at second and third orders for a two-body interaction and a HFB partitioning.

2. Second order perturbations

In addition to different types of interaction, NCPT also facilitates the development of higher-order perturbative approximations. To illustrate this point, we consider here another example. This time, the Hamiltonian and its partitions are defined by

$$\Omega \equiv \Omega_0^{\text{HFB}} + \Omega_1^{\text{HFB}} \tag{75a}$$

where

$$\Omega_0^{\text{HFB}} \equiv \Omega'_0 + \frac{1}{2} \sum_{\mu\nu} U_{\mu\nu} A^\mu A^\nu, \tag{75b}$$

$$\Omega_1^{\text{HFB}} \equiv -\Omega'_0 + \frac{1}{4!} \sum_{\mu_1\mu_2\mu_3\mu_4} v_{\mu_1\mu_2\mu_3\mu_4}^{(2)} A^{\mu_1} A^{\mu_2} A^{\mu_3} A^{\mu_4}. \tag{75c}$$

Here, Ω'_0 is a quadratic Hamiltonian correction to the reference Hamiltonian Ω_0 of Eq. (43). This correction provides the standard HFB partitioning, which we employ here for conciseness. In this particular case, any diagram with a tadpole is cancelled out by the same diagram where the tadpole is replaced by the quadratic perturbation $-\Omega'_0$ [69]. More details on the unperturbed propagator associated to the HFB partitioning are given in Part II. We also assume to have only two-body interactions for simplicity. As a slight abuse of notation, we keep denoting the unperturbed propagator, the quasiparticle energies and the spectroscopic amplitudes respectively as $\mathcal{G}^{(0)\mu\nu}(\omega_e)$, ϵ_n and $X^{(n)\mu}$, $\bar{X}^{(n)\nu}$, although here they are to be understood as those associated to the HFB mean-field.

In this setup, only one diagram contributes to the one-body Green's function at second order, and two, at third order. We show these three diagrams in Fig. 2. The Feynman amplitude $-\mathcal{A}_{(2)}^{\mu\nu}(\omega_m)$ contributing to $\mathcal{G}^{\mu\nu}(\omega_m)$

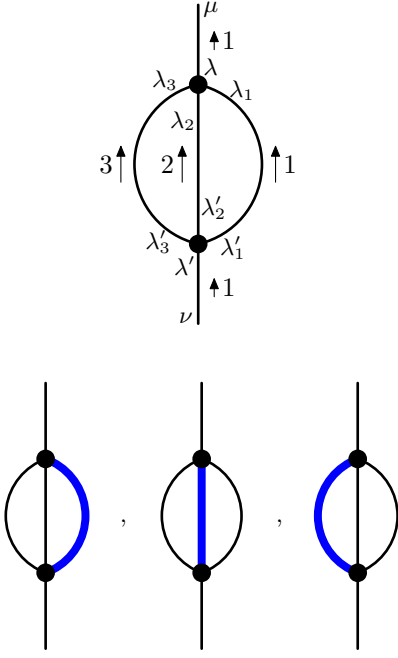


FIG. 3. Top: second-order labelled diagram \mathcal{G}_2 contributing to the propagator. The chosen orientations and strengths are given explicitly. We recall that, by convention, the energy flows positively when following the chosen orientation convention (without taking into account the chosen intensities). Bottom: the three spanning trees of internal lines are shown with bold blue lines. Thin black lines are part of the corresponding complementary diagrams.

at second order reads

$$\begin{aligned}
 -\mathcal{A}_{(2)}^{\mu\nu}(\omega_m) = & \sum_{\lambda\lambda'} \mathcal{G}^{(0)\mu\lambda}(\omega_m) \left\{ \frac{1}{3!} \sum_{\substack{\lambda_1\lambda_2\lambda_3 \\ \lambda'_1\lambda'_2\lambda'_3}} v_{[\lambda\lambda_1\lambda_2\lambda_3]}^{(2)} v_{[\lambda'_3\lambda'_2\lambda'_1\lambda']}^{(2)} \right. \\
 & \times \frac{1}{\beta^2} \sum_{\omega_{l_1}\omega_{l_2}} \left(\mathcal{G}^{(0)\lambda_1\lambda'_1}(\omega_{l_1}) \mathcal{G}^{(0)\lambda_2\lambda'_2}(\omega_{l_2}) \right. \\
 & \left. \left. \mathcal{G}^{(0)\lambda_3\lambda'_3}(\omega_m - \omega_{l_1} - \omega_{l_2}) \right) \right\} \\
 & \times \mathcal{G}^{(0)\lambda'\nu}(\omega_m). \quad (76)
 \end{aligned}$$

The orientation of the energy flow is explicitly shown in the top diagram of Fig. 3. The Matsubara sum $I(\mathcal{G}_2)$ is defined by

$$\begin{aligned}
 I(\mathcal{G}_2) \equiv & \frac{-1}{\beta^2} \sum_{\omega_{l_1}\omega_{l_2}} \mathcal{G}^{(0)\lambda_1\lambda'_1}(\omega_{l_1}) \mathcal{G}^{(0)\lambda_2\lambda'_2}(\omega_{l_2}) \\
 & \times \mathcal{G}^{(0)\lambda_3\lambda'_3}(\omega_m - \omega_{l_1} - \omega_{l_2}). \quad (77)
 \end{aligned}$$

Applying Gaudin's summation rules as given in Sec. III D and App. C, $I(\mathcal{G}_2)$ reads

$$\begin{aligned}
 I(\mathcal{G}_2) = & \sum_{n_1 n_2 n_3} \frac{f(-\epsilon_{n_3})f(-\epsilon_{n_2}) - f(-\epsilon_{n_3})f(\epsilon_{n_1}) + f(\epsilon_{n_2})f(\epsilon_{n_1})}{-i\omega_m + \epsilon_{n_1} + \epsilon_{n_2} + \epsilon_{n_3}} \\
 & \times X^{(n_1)\lambda_1} \bar{X}^{(n_1)\lambda'_1} X^{(n_2)\lambda_2} \bar{X}^{(n_2)\lambda'_2} X^{(n_3)\lambda_3} \bar{X}^{(n_3)\lambda'_3}. \quad (78)
 \end{aligned}$$

Eq. (78) is obtained as the sum of the amplitudes associated to the three spanning trees (bold blue lines) shown in the bottom of Fig. 3. Note that all three trees contribute with the same denominator, which is why only one factorised denominator appears in Eq. (78).

3. Third order perturbations

The simplifications obtained with NCPT become more important as one considers higher perturbative orders. To give a clear illustration, we derive the Feynman amplitudes contributing to the contravariant one-body Green's function at third order. We start with the contribution of the 2PI diagram \mathcal{G}_3 of Fig. 2. The Feynman amplitude $-\mathcal{A}_{(3)}^{\mu\nu}(\omega_m)$ contributing to $\mathcal{G}^{\mu\nu}(\omega_m)$ in this case reads

$$\begin{aligned}
 -\mathcal{A}_{(3)}^{\mu\nu}(\omega_m) = & -\frac{1}{(2!)^2} \sum_{\lambda_1\lambda'_4} \mathcal{G}^{(0)\mu\lambda_1}(\omega_m) \\
 & \times \left\{ \sum_{\substack{\lambda_2\lambda_3\lambda_4 \\ \lambda'_1\lambda'_2\lambda'_3\lambda'_4 \\ \lambda''_1\lambda''_2\lambda''_3}} v_{[\lambda_1\lambda_2\lambda_3\lambda_4]}^{(2)} v_{[\lambda'_4\lambda'_3\lambda'_2\lambda'_1]}^{(2)} v_{[\lambda''_1\lambda''_2\lambda''_3\lambda''_4]}^{(2)} I(\mathcal{G}_3) \right\} \\
 & \times \mathcal{G}^{(0)\lambda'_4\nu}(\omega_m), \quad (79)
 \end{aligned}$$

where $I(\mathcal{G}_3)$ is the Matsubara sum associated to \mathcal{G}_3 , as defined in Eq. (65). The Matsubara sum is computed using Gaudin's summation rules. There are eight spanning trees within \mathcal{G}_3 which are identified in Fig. 4. The associated

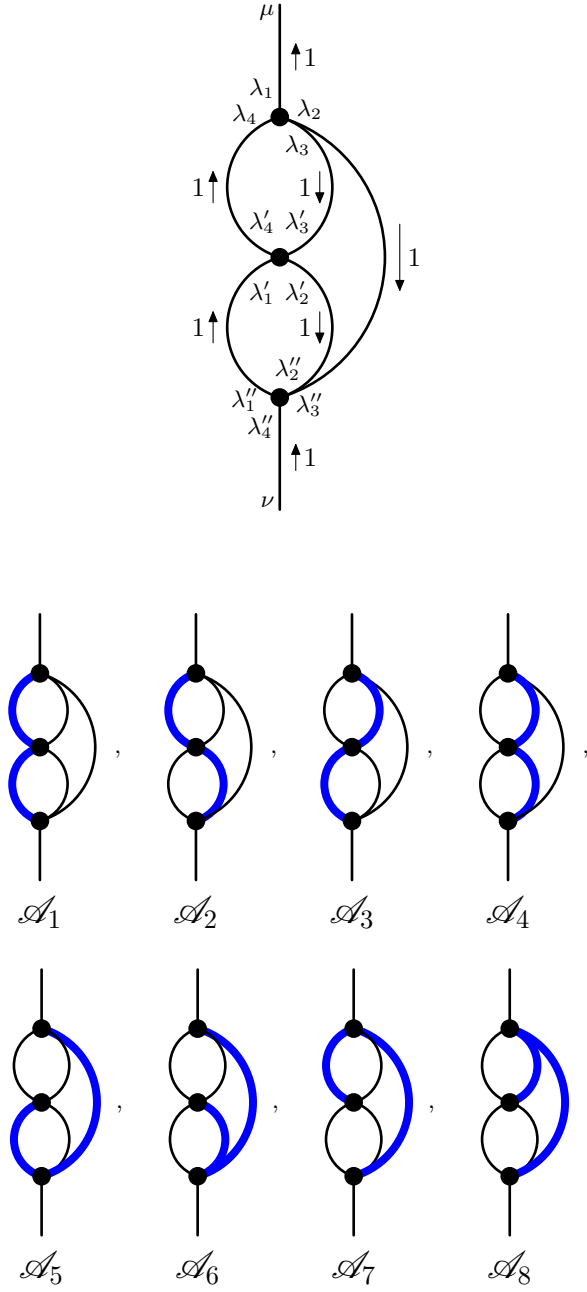


FIG. 4. The same as Fig. 3 for the diagram \mathcal{G}_3 . For this diagram, there are eight distinct spanning trees.

numerators and denominators of each contribution read

$$\mathcal{A}_1 : \frac{f(-\epsilon_{n_2})f(-\epsilon_{n_3})f(-\epsilon_n)}{[-i\omega_m + \epsilon_{n_1} - \epsilon_{n_2} - \epsilon_n][-i\omega_m + \epsilon_{n_4} - \epsilon_{n_3} - \epsilon_n]}, \quad (80a)$$

$$\mathcal{A}_2 : \frac{f(-\epsilon_{n_1})f(-\epsilon_{n_3})f(-\epsilon_n)}{[i\omega_m + \epsilon_{n_2} - \epsilon_{n_1} + \epsilon_n][-i\omega_m + \epsilon_{n_4} - \epsilon_{n_3} - \epsilon_n]}, \quad (80b)$$

$$\mathcal{A}_3 : \frac{f(-\epsilon_{n_2})f(-\epsilon_{n_4})f(-\epsilon_n)}{[-i\omega_m + \epsilon_{n_1} - \epsilon_{n_2} - \epsilon_n][i\omega_m + \epsilon_{n_3} - \epsilon_{n_4} + \epsilon_n]}, \quad (80c)$$

$$\mathcal{A}_4 : \frac{f(-\epsilon_{n_1})f(-\epsilon_{n_4})(-f(\epsilon_n))}{[i\omega_m + \epsilon_{n_2} - \epsilon_{n_1} + \epsilon_n][i\omega_m + \epsilon_{n_3} - \epsilon_{n_4} + \epsilon_n]}, \quad (80d)$$

$$\mathcal{A}_5 : \frac{f(-\epsilon_{n_4})(-f(\epsilon_{n_3}))f(-\epsilon_{n_2})}{[\epsilon_{n_1} - \epsilon_{n_2} + \epsilon_{n_3} - \epsilon_{n_4}][i\omega_m + \epsilon_n + \epsilon_{n_3} - \epsilon_{n_4}]}, \quad (80e)$$

$$\mathcal{A}_6 : \frac{f(-\epsilon_{n_1})f(-\epsilon_{n_4})f(-\epsilon_{n_3})}{[\epsilon_{n_2} - \epsilon_{n_1} + \epsilon_{n_4} - \epsilon_{n_3}][i\omega_m + \epsilon_n + \epsilon_{n_3} - \epsilon_{n_4}]}, \quad (80f)$$

$$\mathcal{A}_7 : \frac{f(-\epsilon_{n_1})(-f(\epsilon_{n_2}))f(-\epsilon_{n_3})}{[\epsilon_{n_4} - \epsilon_{n_3} + \epsilon_{n_2} - \epsilon_{n_1}][i\omega_m + \epsilon_n + \epsilon_{n_2} - \epsilon_{n_1}]}, \quad (80g)$$

$$\mathcal{A}_8 : \frac{f(-\epsilon_{n_1})f(-\epsilon_{n_2})f(-\epsilon_{n_4})}{[\epsilon_{n_3} - \epsilon_{n_4} + \epsilon_{n_1} - \epsilon_{n_2}][i\omega_m + \epsilon_n + \epsilon_{n_2} - \epsilon_{n_1}]}. \quad (80h)$$

The resulting total Matsubara sum reads,

$$\begin{aligned} I(\mathcal{G}_3) = & \sum_{\substack{n_1 n_2 n_3 \\ n_4 n}} X^{(n_1)\lambda'_1} \bar{X}^{(n_1)\lambda'_1} X^{(n_2)\lambda'_2} \bar{X}^{(n_2)\lambda'_2} \\ & \times X^{(n_3)\lambda'_3} \bar{X}^{(n_3)\lambda_3} X^{(n_4)\lambda_4} \bar{X}^{(n_4)\lambda'_4} X^{(n)\lambda'_5} \bar{X}^{(n)\lambda_2} \\ & \times \left\{ \frac{1}{[i\omega_m + \epsilon_{n_2} - \epsilon_{n_1} + \epsilon_n][i\omega_m + \epsilon_{n_3} - \epsilon_{n_4} + \epsilon_n]} \right. \\ & \times [f(-\epsilon_n)f(-\epsilon_{n_2})f(-\epsilon_{n_3}) - f(\epsilon_n)f(-\epsilon_{n_1})f(-\epsilon_{n_4}) \\ & \quad \left. - f(-\epsilon_n)f(-\epsilon_{n_1})f(-\epsilon_{n_3}) - f(-\epsilon_n)f(-\epsilon_{n_2})f(-\epsilon_{n_4})] \right. \\ & + \frac{1}{\epsilon_{n_2} - \epsilon_{n_1} + \epsilon_{n_4} - \epsilon_{n_3}} \\ & \times \left[\frac{f(-\epsilon_{n_4})f(\epsilon_3)f(-\epsilon_{n_2}) + f(-\epsilon_{n_4})f(-\epsilon_3)f(-\epsilon_{n_1})}{i\omega_m + \epsilon_n + \epsilon_{n_3} - \epsilon_{n_4}} \right. \\ & \quad \left. - \frac{f(-\epsilon_{n_1})f(\epsilon_2)f(-\epsilon_{n_3}) + f(-\epsilon_{n_1})f(-\epsilon_2)f(-\epsilon_{n_4})}{i\omega_m + \epsilon_n + \epsilon_{n_2} - \epsilon_{n_1}} \right] \left. \right\} \quad (81) \end{aligned}$$

where denominators have been factorised as done in the second-order case.

The second diagram contributing at third order is a self-energy insertion (that is, of non-skeleton type) and it to be considered two-particle reducible for the application of Gaudin's summation rules of Sec. III D. It is indicated by \mathcal{G}'_3 in Fig. 2. The associated Feynman amplitude

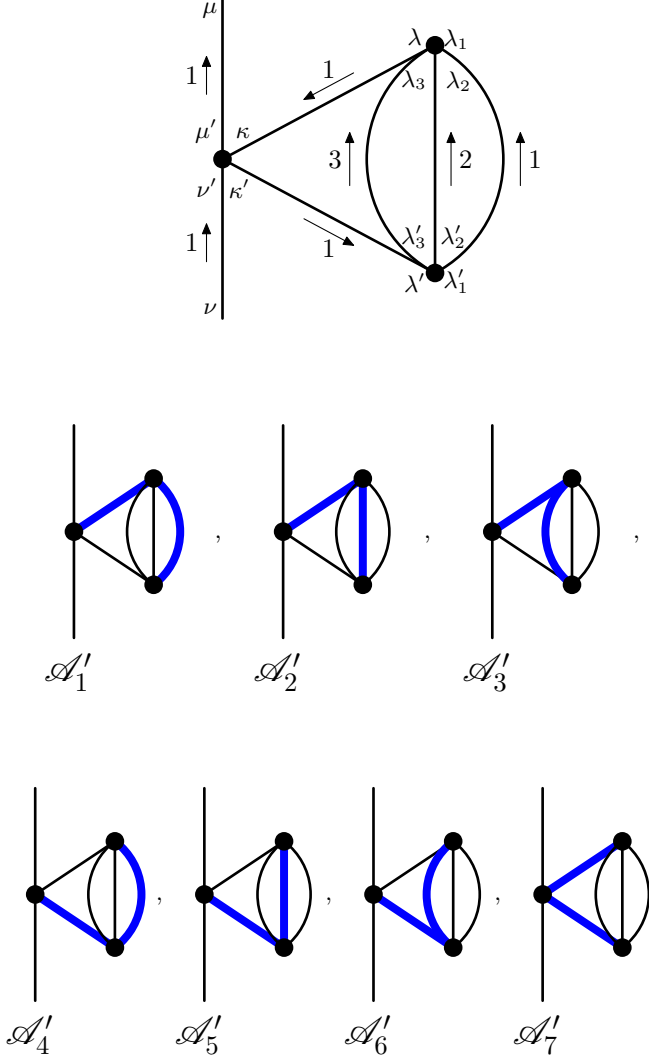


FIG. 5. The same as Fig. 3 for the diagram \mathcal{G}'_3 . For this diagram, there are seven distinct spanning trees.

$-\mathcal{A}_{(3')}^{\mu\nu}(\omega_m)$ reads

$$\begin{aligned}
 -\mathcal{A}_{(3')}^{\mu\nu}(\omega_m) &= -\frac{1}{2 \times 3!} \sum_{\mu'\nu'} \mathcal{G}^{(0)\mu\mu'}(\omega_m) \\
 &\times \left\{ \sum_{\substack{\lambda_1 \lambda_2 \lambda_3 \\ \lambda'_1 \lambda'_2 \lambda'_3 \\ \lambda \lambda' \kappa \kappa'}} v_{[\mu' \kappa \kappa' \nu']}^{(2)} v_{[\lambda \lambda_1 \lambda_2 \lambda_3]}^{(2)} v_{[\lambda'_3 \lambda'_2 \lambda'_1 \lambda']}^{(2)} I(\mathcal{G}'_3) \right\} \\
 &\times \mathcal{G}^{(0)\nu'\nu}(\omega_m), \tag{82}
 \end{aligned}$$

where $I(\mathcal{G}'_3)$ is the associated Matsubara sum. Again, we use Gaudin's summation rules to compute it based on the seven spanning trees of \mathcal{G}'_3 shown in Fig. 5. The

associated numerators and denominators read

$$\mathcal{A}'_1 : \frac{f(-\epsilon_{n_3})f(-\epsilon_{n_2})f(-\epsilon_{n'})}{[\epsilon_{n_1} + \epsilon_{n_2} + \epsilon_{n_3} - \epsilon_{n'}][\epsilon_n - \epsilon_{n'}]}, \tag{83a}$$

$$\mathcal{A}'_2 : \frac{f(-\epsilon_{n_3})(-f(\epsilon_{n_1}))f(-\epsilon_{n'})}{[\epsilon_{n_1} + \epsilon_{n_2} + \epsilon_{n_3} - \epsilon_{n'}][\epsilon_n - \epsilon_{n'}]}, \tag{83b}$$

$$\mathcal{A}'_3 : \frac{(-f(\epsilon_{n_2}))(-f(\epsilon_{n_1}))f(-\epsilon_{n'})}{[\epsilon_{n_1} + \epsilon_{n_2} + \epsilon_{n_3} - \epsilon_{n'}][\epsilon_n - \epsilon_{n'}]}, \tag{83c}$$

$$\mathcal{A}'_4 : \frac{f(-\epsilon_{n_3})f(-\epsilon_{n_2})f(-\epsilon_n)}{[\epsilon_{n_1} + \epsilon_{n_2} + \epsilon_{n_3} - \epsilon_n][\epsilon_{n'} - \epsilon_n]}, \tag{83d}$$

$$\mathcal{A}'_5 : \frac{f(-\epsilon_{n_3})(-f(\epsilon_{n_1}))f(-\epsilon_n)}{[\epsilon_{n_1} + \epsilon_{n_2} + \epsilon_{n_3} - \epsilon_n][\epsilon_{n'} - \epsilon_n]}, \tag{83e}$$

$$\mathcal{A}'_6 : \frac{(-f(\epsilon_{n_2}))(-f(\epsilon_{n_1}))f(-\epsilon_n)}{[\epsilon_{n_1} + \epsilon_{n_2} + \epsilon_{n_3} - \epsilon_n][\epsilon_{n'} - \epsilon_n]}, \tag{83f}$$

$$\mathcal{A}'_7 : \frac{f(-\epsilon_{n_3})f(-\epsilon_{n_2})f(-\epsilon_{n_1})}{[\epsilon_n - \epsilon_{n_1} - \epsilon_{n_2} - \epsilon_{n_3}][\epsilon_{n'} - \epsilon_{n_1} - \epsilon_{n_2} - \epsilon_{n_3}]}. \tag{83g}$$

The resulting Matsubara sum, after factorisation, reads

$$\begin{aligned}
 I(\mathcal{G}'_3) &= \sum_{\substack{n_1 n_2 n_3 \\ n n'}} X^{(n)\kappa} \bar{X}^{(n)\lambda} X^{(n_1)\lambda_1} \bar{X}^{(n_1)\lambda'_1} \\
 &\times X^{(n_2)\lambda_2} \bar{X}^{(n_2)\lambda'_2} X^{(n_3)\lambda_3} \bar{X}^{(n_3)\lambda'_3} X^{(n')\lambda'} \bar{X}^{(n')\kappa'} \\
 &\times \left\{ [f(-\epsilon_{n_3})f(-\epsilon_{n_2}) - f(-\epsilon_{n_3})f(\epsilon_{n_1}) + f(\epsilon_{n_2})f(\epsilon_{n_1})] \right. \\
 &\quad \times \left[\frac{f(-\epsilon_{n'})}{\epsilon_{n_1} + \epsilon_{n_2} + \epsilon_{n_3} - \epsilon_{n'}} - \frac{f(-\epsilon_n)}{\epsilon_{n_1} + \epsilon_{n_2} + \epsilon_{n_3} - \epsilon_n} \right] \\
 &\quad \left. + \frac{f(-\epsilon_{n_3})f(-\epsilon_{n_2})f(-\epsilon_{n_1})}{[\epsilon_n - \epsilon_{n_1} - \epsilon_{n_2} - \epsilon_{n_3}][\epsilon_{n'} - \epsilon_{n_1} - \epsilon_{n_2} - \epsilon_{n_3}]} \right\}. \tag{84}
 \end{aligned}$$

4. Discussion

Eqs. (78), (81) and (84) provide three relatively compact and straightforward expressions for the second and third order contributions of the one-body propagator. The denominator factorisation in these expressions is possible whenever the denominators are associated to spanning trees differing only in the choice of equivalent lines. At second order only one class of trees appears. At third order, for each diagram, only three different classes appear. Deriving general rules to get directly fully factorised amplitudes would be interesting, in order to get optimal algebraic formula ready to be implemented numerically. Those rules may also mitigate the increasing number of spanning trees with perturbative order since, in general, only one member of each class of trees needs to be considered. Such refinements are beyond the scope of this article and are left for future developments.

As discussed earlier, infrared divergences may appear in the form of vanishing denominators of separate spanning tree contributions. We have chosen to write Eq. (84) in

a form which manifestly highlights the cancellation of the infrared divergence associated to the denominator $[\epsilon_n - \epsilon_{n'}]$ for different spanning trees. In this case, we find two denominators that differ only in the exchange $\epsilon_n \leftrightarrow \epsilon_{n'}$. Expanding the term that depends on $\epsilon_{n'}$ around ϵ_n , and taking the limit $\epsilon_{n'} \rightarrow \epsilon_n$, one finds

$$\begin{aligned} & \lim_{\epsilon_{n'} \rightarrow \epsilon_n} \left[\frac{\frac{f(-\epsilon_{n'})}{\epsilon_{n_1 + \epsilon_{n_2} + \epsilon_{n_3} - \epsilon_{n'}} - \frac{f(-\epsilon_n)}{\epsilon_{n_1 + \epsilon_{n_2} + \epsilon_{n_3} - \epsilon_n}}}{\epsilon_n - \epsilon_{n'}} \right] \\ &= \frac{f'(-\epsilon_n)}{\epsilon_{n_1} + \epsilon_{n_2} + \epsilon_{n_3} - \epsilon_n} - \frac{f(-\epsilon_n)}{[\epsilon_{n_1} + \epsilon_{n_2} + \epsilon_{n_3} - \epsilon_n]^2}, \end{aligned} \quad (85)$$

where f' denotes the derivative of the Fermi-Dirac distribution. Similarly, one could consider the case where $[\epsilon_n - \epsilon_{n'}]$ and $[\epsilon_{n_1} + \epsilon_{n_2} + \epsilon_{n_3} - \epsilon_n]$ are simultaneously vanishing. We have checked that the double limit $\lim_{\epsilon_n \rightarrow (\epsilon_{n_1} + \epsilon_{n_2} + \epsilon_{n_3})} \lim_{\epsilon_{n'} \rightarrow \epsilon_n}$ of the Matsubara sum is well-defined also in this case. In general, the Matsubara sum is absolutely convergent¹⁰ so that $I(\mathcal{G})$ is always finite. Thus, any divergence occurring in the sum over quasiparticle energies for a particular $I(\mathcal{A})$ is artificial and it necessarily cancels out when combined with contributions from different spanning trees.

In this section we have derived explicitly several perturbative contributions to the contravariant one-body Green's function. Remarkably, the Nambu-covariant formalism used in the formulation of NCPT allows to obtain very compact expressions. We have been able to showcase the full third order contribution in the case of a HFB partitioning and an Hamiltonian with a two-body interaction. At the same time, we have shown that the Nambu-covariant formalism allows to easily derive the first order contribution to the contravariant one-body Green's function with arbitrarily high k -body interactions. However, perturbative contributions are in some cases insufficient. Relevant approximations for several physical systems, such as strongly correlated fermions, require non-perturbative summations of subsets of diagrams. Such infinite summations are addressed in Part II, where we discuss self-consistently dressed propagators and vertices in the Nambu-covariant formalism.

¹⁰ This is due to the fact that any independent Matsubara frequency appears at least in two different propagators except for frequencies associated to tadpoles. Each propagator is an $O(\omega_i^{-1})$ function, such that the sequence that is summed over in Eq. (67) is of $O(\omega_i^{-2})$, and the series converges absolutely. The particular case of the tadpole, as usual, is taken care of by the regularising η -term coming out of Feynman rules.

IV. CONNECTION WITH STANDARD FORMALISMS

The contravariant many-body Green's functions and the un-oriented Feynman diagrams are fundamental objects of the Nambu-covariant formalism. To clarify their meaning we discuss their relation with their counterpart appearing in the more standard Gorkov and Bogoliubov formalisms.

A. Gorkov formalism

Let us first make the connection with the Gorkov formalism as discussed extensively, for nuclear physics applications, in Ref. [5]. To do so, we consider the orthonormal single-particle bases \mathcal{B} and $\tilde{\mathcal{B}}$ related by the bijection $\tilde{\cdot}$ defined by

$$\tilde{\cdot} : |a\rangle \mapsto |\tilde{a}\rangle \equiv \eta_a |\hat{a}\rangle, \quad (86)$$

where η_a is a phase factor and $\hat{\cdot}$ an involution on the elements of \mathcal{B} as defined in Ref. [5]¹¹. We also consider the Hamiltonian to be Hermitian and reading

$$\Omega \equiv \sum_{bc} T_{bc} a_b^\dagger a_c + \frac{1}{(2!)^2} \sum_{bcde} \bar{V}_{bcde} a_b^\dagger a_c^\dagger a_e a_d. \quad (87)$$

To make the connection with the Gorkov formalism transparent, we work in the extended basis

$$\mathcal{B}^{e'} = \mathcal{B} \cup \tilde{\mathcal{B}}^\dagger \quad (88)$$

which is related to the standard extended basis

$$\mathcal{B}^e = \mathcal{B} \cup \mathcal{B}^\dagger \quad (89)$$

by a non-canonical transformation. Their respective Nambu fields A'^{μ} and A^μ are related according to the transformation of Eqs. (21) with

$$\mathcal{W}^{(b,l_b)}_{(c,l_c)} \equiv \begin{pmatrix} 1 & 0 \\ 0 & \eta_c^{-1} \delta_{\tilde{b}c} \end{pmatrix}_{l_b l_c}, \quad (90)$$

where the sub-indices $l_b l_c$ means that the 2×2 matrix is to be evaluated at those Nambu indices. Explicitly, the Nambu fields associated to $\mathcal{B}^{e'}$ read¹²

$$A'^{(b,1)} = a_b, \quad (91a)$$

$$A'^{(b,2)} = \bar{a}_{\tilde{b}} = a_{\tilde{b}}^\dagger, \quad (91b)$$

$$\bar{A}'_{(b,1)} \equiv \bar{a}_b = a_b^\dagger, \quad (91c)$$

$$\bar{A}'_{(b,2)} \equiv a_{\tilde{b}}. \quad (91d)$$

¹¹ To avoid a conflict of notations, the bijection between elements of \mathcal{B} and $\tilde{\mathcal{B}}$ has been renamed $\tilde{\cdot}$, whereas the notation $\bar{\cdot}$ is used in Ref. [5]. The latter would clash with our previous use of $\bar{\cdot}$ to denote the dual basis. The involution on \mathcal{B} has been renamed $\hat{\cdot}$, while $\tilde{\cdot}$ is used in Ref. [5].

¹² Here, the single-particle bases \mathcal{B} and $\tilde{\mathcal{B}}$ are assumed to be orthonormal. Hence, the associated creation and annihilation operators are Hermitian conjugated to each other.

In terms of the Nambu fields A'^{μ} , the Hamiltonian reads

$$\Omega = \frac{1}{2!} \sum_{\mu_1 \mu_2} t_{\mu_1 \mu_2} A'^{\mu_1} A'^{\mu_2} + \frac{1}{4!} \sum_{\mu_1 \mu_2 \mu_3 \mu_4} v_{\mu_1 \mu_2 \mu_3 \mu_4}^{(2)} A'^{\mu_1} A'^{\mu_2} A'^{\mu_3} A'^{\mu_4}. \quad (92)$$

Working in the particular extended basis $\mathcal{B}^{e'}$, the relationship between the contravariant many-body Green's functions and the many-body Green's functions as devised in Ref. [5] straightforwardly reads

$$(-1)^k \mathcal{G}^{(b_{1,1}) \dots (b_{2k,1})}(\tau_1, \dots, \tau_{2k}) = \langle \text{T} [a_{b_1}(\tau_1) \dots a_{b_{2k}}(\tau_{2k})] \rangle, \quad (93a)$$

$$(-1)^k \mathcal{G}^{(b_{1,2}) (b_{2,1}) \dots (b_{2k,1})}(\tau_1, \dots, \tau_{2k}) = \left\langle \text{T} \left[a_{b_1}^\dagger(\tau_1) a_{b_2}(\tau_2) \dots a_{b_{2k}}(\tau_{2k}) \right] \right\rangle, \quad (93b)$$

\vdots

$$(-1)^k \mathcal{G}^{(b_{1,2}) (b_{2,2}) \dots (b_{2k,2})}(\tau_1, \dots, \tau_{2k}) = \left\langle \text{T} \left[a_{b_1}^\dagger(\tau_1) a_{b_2}^\dagger(\tau_2) \dots a_{b_{2k}}^\dagger(\tau_{2k}) \right] \right\rangle. \quad (93c)$$

In principle, there are 2^{2k} different k -body Green's functions, counting both anomalous and normal ones. Using the Hermitian symmetry of the Hamiltonian and the antisymmetry of the time-ordering, the number of independent k -body Green's functions reduces to $k+1$. It is clear that if one is interested in high- k many-body Green's functions, working with the unique tensor Green's function defined in Eq. (45) is much more convenient than having to consider, separately, its $k+1$ independent components.

Let us now relate the amplitude of an un-oriented diagram \mathcal{G} to the amplitudes associated to Gorkov diagrams as defined in Ref. [5]. It is straightforward to verify that a given un-oriented diagram \mathcal{G} with *fixed* Nambu indices on its line, reduces to one oriented diagram of the Gorkov diagrammatic, up to a prefactor. Indeed, we clearly see from Eqs. (52) and Eqs. (93) that fixing Nambu indices amounts to fixing the kind of Gorkov propagators (normal or anomalous) appearing in the amplitude of the diagram. Then, as detailed in App. B2, the totally antisymmetric vertex $v_{[\lambda_1 \lambda_2 \lambda_3 \lambda_4]}^{(2)}$ at fixed Nambu indices, reduces to a particular matrix element of type \bar{V}_{bcde} . This is clearly seen from Eq. (B17). Eventually, the amplitude of an un-oriented Feynman diagram with fixed Nambu indices is a sum of a product of standard matrix elements of the potential and normal/anomalous propagators, all contracted on single-particle indices according to the topology of the un-oriented diagram. Fixing Nambu indices on an un-oriented diagram thus leads to a contribution proportional to the amplitude of a Gorkov diagram whose topology is the same as the un-oriented diagram and whose orientation is dictated by the fixed Nambu indices. This particular Gorkov diagram is said to be associated to the fixing of Nambu indices.

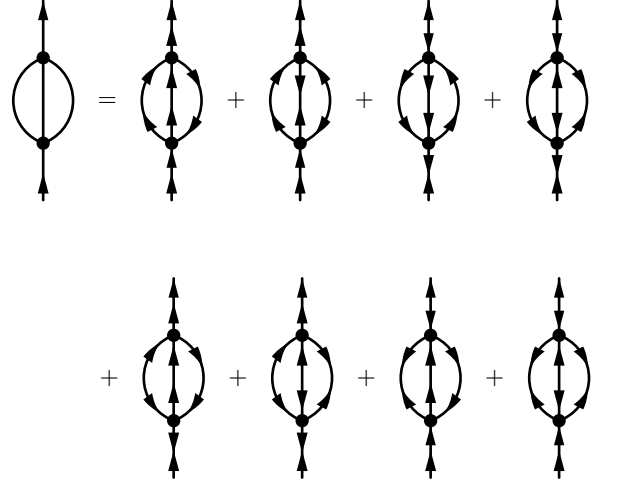


FIG. 6. Gorkov diagrams factorised in the second order un-oriented diagram for a given set of fixed external Nambu indices. The fixed Nambu indices are represented by external arrows on the original un-oriented diagram.

One should be careful that fixing Nambu indices, however, *does not* give directly the amplitude of a Gorkov diagram. Several sets of fixed Nambu indices can have the same associated Gorkov diagram. Only when summing over all the sets of Nambu indices associated to a given Gorkov diagram one will recover its full amplitude. A proper proof of this statement is beyond the scope of this article. The most delicate point is to check that the right symmetry factor is recovered when summing over all sets of fixed Nambu indices associated to one Gorkov diagram¹³.

As a consequence of this statement, an un-oriented diagram with fixed external Nambu indices equals the sum of all Gorkov diagrams obtained by orienting the diagram in a compatible way with the fixed external Nambu indices. We have explicitly checked this for the first and second order expansion of the one-body Green's function. We refer to this relation as a factorisation of Gorkov diagrams. An example of such factorisation at second order is shown in Fig. 6. Let us denote the number of Gorkov diagrams factorised in a given un-oriented diagram \mathcal{G} (at fixed external Nambu indices) by $F_{\text{Gorkov}}(\mathcal{G})$. A naive upper bound on the number of diagrams factorised consists in counting all possible orientations, i.e.

$$F_{\text{Gorkov}}(\mathcal{G}) \leq 2^{2(I+k)}, \quad (94)$$

where I and $2k$ are respectively the number of internal and external lines of \mathcal{G} . We can refine this upper bound by

¹³ This point is subtle because several sets of Nambu indices might lead to several topologically equivalent Gorkov diagrams. This is typically the case when fixing Nambu indices of equivalent lines. This can also occur when several sets of fixed Nambu indices lead to the same Gorkov diagram up to a permutation of vertices.

taking into account the fact that the potential is particle-number conserving. Let us assume that only interactions up to k_{\max} -body are considered. As a consequence, only orientations where k_i incoming and k_i outgoing arrows occur at each k_i -body vertex give a non-zero contribution. Instead of counting orientations of lines we count orientations of vertices which are limited to $\binom{2k_i}{k_i}$ instead of 2^{2k_i} . For an un-oriented diagram \mathcal{G}_n (at fixed external Nambu indices) with n vertices, we get the refined upper bound

$$F_{\text{Gorkov}}(\mathcal{G}_n) \leq \binom{2k_{\max}}{k_{\max}}^n. \quad (95)$$

We estimate that the number of factorised Gorkov diagrams grows exponentially with n . Let us stress that this estimate does not take into account the topology of the diagram. For example, two different orientations of the vertices might lead to the same Gorkov diagram up to a permutation of equivalent lines. Taking into account such double counting would partially reduce the estimate, nevertheless we expect the exponential growth with the number of vertices to hold in general.

B. Bogoliubov formalism

We now consider the connection between the Nambu-covariant formalism and the Bogoliubov formalism discussed in Refs. [6, 51]. We focus on the perturbative version of the formalisms, namely NCPT and Bogoliubov many-body perturbation theory (BMBPT) [70]. The latter relies on quasiparticle creation and annihilation operators related to single-particle creation and annihilation operators obtained by the unitary Bogoliubov transformation

$$\beta_k \equiv \sum_b U_{bk}^* a_b + V_{bk}^* a_b^\dagger, \quad (96a)$$

$$\beta_k^\dagger \equiv \sum_b U_{bk} a_b + V_{bk} a_b^\dagger, \quad (96b)$$

where quasiparticle states are indexed over k indices and where single-particle states are those of an orthonormal basis \mathcal{B} indexed over b indices. The Bogoliubov formalism developed in Refs. [6, 51, 70] focuses mainly on the case where the Hamiltonian is partitioned as

$$\Omega \equiv \Omega_0 + \Omega_1, \quad (97a)$$

$$\Omega_0 \equiv \Omega^{00} + \bar{\Omega}^{11}, \quad (97b)$$

$$\begin{aligned} \Omega_1 \equiv & \Omega^{20} + \check{\Omega}^{11} + \Omega^{02} \\ & + \Omega^{40} + \Omega^{31} + \Omega^{22} + \Omega^{13} + \Omega^{04}, \end{aligned} \quad (97c)$$

where Ω^{00} is proportional to the identity and $\bar{\Omega}^{11}$ is diagonal, i.e.

$$\Omega^{00} \propto \mathbb{1}_{\mathcal{F}}, \quad (98a)$$

$$\bar{\Omega}^{11} \equiv \sum_k E_k \beta_k^\dagger \beta_k, \quad (98b)$$

with $E_k > 0$. For such partitioning the unperturbed propagator contains only normal components (with respect to quasiparticle creation and annihilation operators). We also use the shorthand notation Ω^{ij} to denote an operator involving i quasiparticle creation operators and j quasiparticle annihilation operators, i.e. for example

$$\Omega^{31} \equiv \frac{1}{3!} \sum_{k_1 k_2 k_3 k_4} \Omega_{k_1 k_2 k_3 k_4}^{31} \beta_{k_1}^\dagger \beta_{k_2}^\dagger \beta_{k_3}^\dagger \beta_{k_4}. \quad (99)$$

This reformulation allows to exchange anomalous lines in Gorkov diagrammatics with anomalous vertices in Bogoliubov diagrammatics [61]. Here, by anomalous vertices we mean vertices where the number of incoming lines does not necessarily match the number of outgoing lines.

To connect NCPT and BMBPT, we start from the extended basis $\mathcal{B}^e = \mathcal{B} \cup \mathcal{B}^\dagger$, where now \mathcal{B} is the same orthonormal single-particle basis used in Eqs. (96). We then perform the same unitary Bogoliubov transformation as in Eqs. (96) to perform a change of extended basis from \mathcal{B}^e to $\mathcal{B}^{e'} \equiv \{|(k, l_k)\rangle\}$ indexed over quasiparticle and Nambu indices. The new Nambu fields are thus defined by Eqs. (21), with the transformation

$$\mathcal{W}^{(b, l_b)}_{(k, l_k)} \equiv \begin{pmatrix} U_{bk} & V_{bk}^* \\ V_{bk} & U_{bk}^* \end{pmatrix}_{l_b l_k}. \quad (100)$$

In this case, the new Nambu fields read¹⁴

$$A'^{(k,1)} = \beta_k, \quad (101a)$$

$$A'^{(k,2)} = \bar{\beta}_k = \beta_k^\dagger, \quad (101b)$$

$$\bar{A}'_{(k,1)} \equiv \bar{\beta}_k = \beta_k^\dagger, \quad (101c)$$

$$\bar{A}'_{(k,2)} \equiv \beta_k. \quad (101d)$$

The connection between BMBPT and NCPT diagrammatics, expressed in terms of Nambu fields A'^{μ} , follows in a similar fashion as for the Gorkov case. The main difference is that, this time, only normal lines occur and anomalous vertices are allowed. Many-body Green's functions are related to the contravariant ones with fixed Nambu indices. Un-oriented diagrams with fixed external Nambu indices are then again related to the sum of all possible orientations. We refer to this relationship between diagrams as a factorisation of Bogoliubov diagrams. An example of such factorisation is given in Fig. 7. Similarly to the Gorkov case, we denote the number of Bogoliubov diagrams factorised in a given un-oriented diagram \mathcal{G} by $F_{\text{Bogoliubov}}(\mathcal{G})$. This time, the upper bound on $F_{\text{Bogoliubov}}(\mathcal{G})$ which takes into account the fact that only normal lines are allowed reads

$$F_{\text{Bogoliubov}}(\mathcal{G}) \leq 2^I, \quad (102)$$

¹⁴ Since the single-particle basis \mathcal{B} is orthonormal and the Bogoliubov transformation is unitary, the creation/annihilation operators associated to the new Nambu fields are Hermitian conjugated to each other. For more details on unitary Bogoliubov transformations see App. A of Part II.

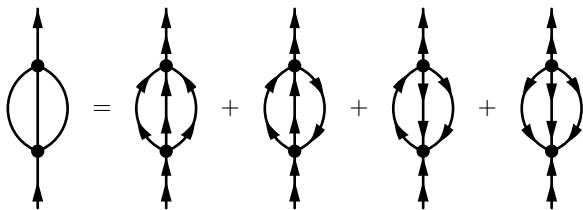


FIG. 7. Bogoliubov diagrams factorised in the second order un-oriented diagram for a given set of fixed external Nambu indices. The fixed Nambu indices are represented by external arrows on the original un-oriented diagram. Pay attention that diagrams containing directed cycles are not discarded at non-vanishing temperatures, contrary to a common selection rule derived in the zero temperature formalism of Ref. [51].

where I is the number of internal lines of \mathcal{G} . We estimate that the number of factorised Bogoliubov diagrams grows exponentially with I . Let us stress again that this estimate does not take into account the topology of the diagram. For example, two different orientations of the lines could lead to the same Bogoliubov diagram up to a permutation of equivalent lines. Taking into account such double counting would reduce the estimate. Again, we expect the exponential growth with the number of internal lines to hold, provided the number of vertices also grows¹⁵.

C. Nambu-invariance and truncations

Let us consider a many-body approximation defined as a truncation on the set of un-oriented diagrams contributing to the many-body Green's functions. Since any diagram is a tensor of the same nature as the Green's function to which it contributes, the approximated Green's functions are guaranteed to conserve their tensor character. Let $\mathcal{G}_{\text{MB}}^{\mu_1 \dots \mu_{2k}}(\tau_1, \dots, \tau_{2k})$ be the approximated k -body Green's functions, and O be a k -body observable such that

$$O = \sum_{\mu_1 \dots \mu_{2k}} o_{\mu_1 \dots \mu_{2k}} A^{\mu_1} \dots A^{\mu_{2k}}. \quad (103)$$

The approximated expectation value of the observable is defined as

$$\langle O \rangle_{\text{MB}} \equiv (-1)^k \sum_{\mu_1 \dots \mu_{2k}} o_{\mu_1 \dots \mu_{2k}} \mathcal{G}_{\text{MB}}^{\mu_1 \dots \mu_{2k}}(0^{+\dots+}, \dots, 0), \quad (104)$$

where the zero-time limit is to be understood as taken while keeping $\tau_1 > \dots > \tau_{2k}$. As long as

$\mathcal{G}_{\text{MB}}^{\mu_1 \dots \mu_{2k}}(\tau_1, \dots, \tau_{2k})$ is a $(2k, 0)$ -tensor at any fixed set of times, the approximated expectation value $\langle O \rangle_{\text{MB}}$ will be a type $(0, 0)$ (or scalar) tensor. Consequently, the approximated expectation value is not only single-particle invariant but also *Nambu invariant* which includes, as a sub-case, the invariance with respect to any Bogoliubov transformation.

This invariance property of the approximated observables is *not* guaranteed when considering many-body approximations defined by a set of Gorkov or Bogoliubov diagrams. In general, Gorkov or Bogoliubov diagrammatic contributions that differ only by their orientations are reshuffled when performing a Bogoliubov transformation or, more generally, when performing a change of extended basis. In other words, the invariance under transformations of an approximated observable is only recovered when the set of diagrams defining the approximation contains *all* the possible orientations of each diagram it contains. As it was discussed in Secs. IV A and IV B, such a many-body approximation can be expressed as a truncation on the set of un-oriented diagrams obtained from NCPT and $\langle O \rangle_{\text{MB}}$ is a scalar tensor. This is the case, for example, of the recent and successful many-body approximations referred to as BMBPT(n) in Ref. [70], which include all Bogoliubov diagrams containing up to n vertices.

Ensuring that the many-body approximation considered is Nambu invariant is not only desirable from a purely theoretical point of view. We expect that invariance will also have an impact on numerical efficiency. In the case of truncated model space calculations, Nambu invariance ensures the crucial property that the complete basis set limit is independent from the extended basis chosen to implement the calculations. Such extended basis independence opens the way towards further optimisations. For instance, the extended basis can be chosen to maximise the reliability and speed of convergence towards the complete basis set limit. Such basis optimisation strategies have been studied at length in quantum chemistry, see Ref. [71] for a recent review. Basis optimisation was recently shown to be of great importance for successful large-scale calculations of nuclear structure observables [72–74]. So far, only invariance with respect to the choice of single-particle basis has been considered, with a focus on symmetry-conserving calculations. Nambu-invariant many-body approximations could benefit greatly from further prospects in the optimisation of the extended basis, although it is not yet immediate to give *a priori* arguments for preferring a certain extended basis over another. An optimised extended basis \mathcal{B}^e might be of Gorkov type (i.e. taking advantage of particle-number conservation at vertices by using an extended basis based on single-particle states), of Bogoliubov type (i.e. taking advantage of a diagonal propagator by using an extended basis based on quasiparticle states) or, actually, anything else. The virtue of the NCPT developed in this article is that it remains unbiased with respect to the chosen extended basis \mathcal{B}^e , allowing for a large range of potential

¹⁵ Heuristically, the growth of the number of vertices is essential to avoid saturation of vertices, i.e. to avoid being in a situation where any additional internal line is also an additional equivalent line. This worst case scenario is avoided if we assume to have only up to k_{max} -body interaction since at some point adding new internal lines will require adding new vertices.

optimisation strategies.

Last but not least, let us briefly discuss the diagrammatic factorisation mentioned in Secs. IV A and IV B and its potential impact on numerical efficiency. At first sight, factorisation may appear to be an artifice recasting several standard diagrams into a single un-oriented diagram at the price of doubling the dimension of the one-body space, from \mathcal{H}_1 to the one of \mathcal{H}_1^e . Working with un-oriented diagrams has, nonetheless, two *a priori* main advantages. The first benefit is formal: one can work with tensors with a greater degree of symmetry than in other approaches, such as $v_{[\mu_1 \dots \mu_{2k}]}^{(k)}$, which is totally antisymmetric. This suggests that the increase in size of the model space can be (at least partly) mitigated by the additional symmetries in the evaluation of the tensor network. The second benefit is specific to numerical implementations on massively parallel hardware: a greater degree of parallelisation of the floating-point operations is exposed in NCPT equations, without increasing data movements. This is a general consequence of replacing several different tensor contractions by a unique one, with larger dimensions. Parallelising floating-point operations without increasing data movements is key to increase efficiency of GPU-based architectures [55]¹⁶. Therefore, we expect that trading a smaller set of tensor networks for a larger model space will increase the gain obtained by using accelerator hardware, such as GPUs. We stress that accelerators are becoming more and more important in the numerical evaluation of tensor networks, thanks to the rapidly growing software infrastructures deploying more efficient and easier-to-use algorithms [55, 56]. Taking advantage of these developments to their fullest potential is a point that should not be neglected. We are aware that this discussion is purely qualitative, and the practical benefits remain speculative at this point. Ultimately, one would have to develop quantitative studies which will likely depend on the many-body problem and the computational resources at stake.

V. CONCLUSIONS

Since the development of a microscopic theory of superconductivity by Bardeen, Cooper and Schrieffer [1, 2] several reformulations of symmetry-broken many-body theory have occurred. Nambu's original reformulation was based on so-called Nambu fields [11], and used the fact that these fields respect the usual canonical anti-commutation rules which, in the notation of this paper,

read

$$\{ A^\mu, \bar{A}_\nu \} = \delta_{\mu\nu} . \quad (105)$$

This property allowed Nambu to develop a perturbation theory based on oriented Feynman diagrams free of anomalous lines, but where propagators are 2×2 matrices. Whether working with a matrix propagator or with separate normal and anomalous propagators, a commonly used shorthand notation has been to denote by un-oriented diagrams the sum of their oriented versions, compatible with the Feynman rules to be employed. In such approaches, the non-trivial dependence of the amplitudes on Nambu indices precludes a clear factorisation of the different orientations of a given diagram. To the best of our knowledge, a reformulation of Feynman diagrammatics verifying the requirement that Nambu indices only impact the value of a diagram via their contractions in a tensor network was first introduced by De Dominicis and Martin [13, 14]. The key basis for this formulation is that it expresses the many-body problem solely in terms of contravariant Nambu fields, A^μ , despite having

$$\{ A^\mu, A^\nu \} = g^{\mu\nu} \neq \delta_{\mu\nu} . \quad (106)$$

Later on, diagrammatics with the same property were independently reintroduced by Kleinert [15, 16] and Haussmann [17, 18]. These approaches are all based on diagrams with un-oriented lines and totally antisymmetric vertices, going beyond the traditional Hugenholtz antisymmetrisation.

In the present work, previous reformulations have been taken further by extending them to a general Hamiltonian expressed in a general extended basis. The success of such reformulation has been shown to be underpinned by the algebraic structure of Nambu tensors, detailed in Sec. II. The covariance and contravariance of Nambu tensors was defined to be with respect to any change of extended basis. These include, as a sub-case, changes of single-particle basis; unitary and non-unitary Bogoliubov transformations; and an additional set of non-canonical linear transformations, i.e. transformations modifying the metric $g_{\mu\nu}$. The perturbation theory resulting from working in the Nambu-covariant formalism, dubbed Nambu-Covariant Perturbation Theory, deals with two- and many-body interactions; it is conceived explicitly at non-zero temperature; and it eventually results in simplified un-oriented Feynman diagrammatics with fully antisymmetrised interaction vertices.

In Secs. III B and III C, we give the Feynman rules that provide an expansion of the (contravariant) many-body Green's functions. The un-oriented Feynman diagrams appearing in the perturbative expansion decompose the many-body Green's functions in terms of Nambu tensors. Let us also stress two particular subtleties appearing in NCPT. The first, which did not appear in previous works [13–18], is the partial antisymmetrisation of interaction vertices, which is required when tadpoles are contracted over them. This is necessary unless we assume

¹⁶ To emphasise the importance of reducing data movements, let us stress that the reading (writing) bandwidth between CPUs and GPUs ranges, for a modern standard, from 16 GB/s (for 8 reading (writing) lanes of a 4th generation PCI Express) to 150 GB/s (for 48 reading (writing) lanes of 2nd generation NVlink), while the computational power of a GPU ranges between 1 Tflop/s and 10 Tflop/s (e.g. for a NVIDIA K20 and V100 GPU).

the components $v_{\mu_1 \dots \mu_{2k}}^{(k)}$ to be totally antisymmetric from the start. Although such decomposition of the Hamiltonian is in general possible, it might not be optimal for numerical applications. The second subtlety is the almost, but not quite, direct connection between the NCPT diagrammatics for fixed external Nambu indices, and the more standard Gorkov and Bogoliubov diagrammatics, discussed in Secs. IV A and IV B.

Although the developments of NCPT in Sec. III are restricted to the single-reference case, we work in a general enough setting that could be of interest for further extensions. In particular, we leave open the possibility of working with an extended basis built upon a non-orthogonal single-particle basis, as in Eq. (5). Our formalism can also deal with non-Hermitian unperturbed Hamiltonians. These two advantages (a non-orthogonal basis, diagonalising a non-Hermitian unperturbed Hamiltonian) should be useful in applications to certain flavours of multi-reference perturbation theory. For instance, let us mention the multi-configuration perturbation theory (MCPT) [75] which has recently been applied to open-shell nuclei [76]; or the non-orthogonal configuration interaction with second-order perturbation theory built on top (NOCI-PT2), which has been recently developed and applied in quantum chemistry [77]. Our general setting may also be useful in the developments of projected Bogoliubov many-body perturbation theory (PBMBPT) [51]. In this case, at zero temperature, spontaneously broken symmetries are restored by mixing several single-reference calculations over vacua which differ by a non-unitary Bogoliubov transformation. While such developments lie beyond the scope of this work, it would be interesting to study how the Nambu-covariant formalism could be used to reformulate the above approaches and see if any formal simplifications or numerical optimisations arise. Beyond formal and numerical improvements, the ability to handle non-Hermitian Hamiltonians and their non-orthogonal basis is also important phenomenologically for applications to open quantum systems. For example, the description of nuclear reactions relies crucially on effective Hamiltonians arising from a Feshbach projection [78]. These effective Hamiltonians are, in general, non-Hermitian. We refer the reader to Ref. [79] for a recent review on non-Hermitian Hamiltonians and their physical applications.

To conclude, the focus of this work has been on the perturbative aspects of many-body theory and how they can be formulated in a Nambu-covariant fashion. In the case of a physical system made of strongly correlated fermions, perturbative approximations may be insufficient. One avenue to solve this problem consists in dressing propagators and vertices using advanced many-body techniques in order to effectively sum infinite sets of diagrams. In Part II of this work, we consider infinite summations of diagrams obtained via self-consistently dressed propagators and vertices in a Nambu-covariant fashion [54]. The mere fact that these additional considerations are possible is proof of the versatility and potentiality of this new Nambu-covariant formalism.

ACKNOWLEDGMENTS

The authors thank J. W. T. Keeble for proofreading the manuscript. M. D. would like to acknowledge useful discussions and comments with the nuclear theory group of CEA-Saclay on an earlier version of this work.

This work is supported by STFC, through Grants Nos ST/L005743/1 and ST/P005314/1; by the Spanish MICINN through the ‘‘Ram3n y Cajal’’ program with grant RYC2018-026072 and the ‘‘Unit of Excellence Mar3a de Maeztu 2020-2023’’ award to the Institute of Cosmos Sciences (CEX2019-000918-M).

Appendix A: Matrix elements

In this appendix, we relate the standard expression of a k -body operator to its fully covariant representation. In practical applications, one will need to perform a transformation from the standard operator matrix elements into the fully covariant tensor coordinates appearing in the Nambu-covariant formalism. For a fixed single-particle basis, this transformation should be a one-off (pre-processing) step before fully-fledged many-body steps are developed.

For a given choice of single-particle basis \mathcal{B} , a k -body operator O reads, in general,

$$O \equiv \sum_{\substack{b_1 \dots b_k \\ c_1 \dots c_k}} o_{b_1 \dots b_k c_1 \dots c_k} \bar{a}_{b_1} \dots \bar{a}_{b_k} a_{c_k} \dots a_{c_1}, \quad (\text{A1})$$

where $o_{b_1 \dots b_k c_1 \dots c_k}$ are generic complex numbers. Similarly, for a given extended basis \mathcal{B}^e , the operator reads, in terms of a mixed (k, k) -tensor of coordinates $o^{\mu_1 \dots \mu_k}_{\mu_{k+1} \dots \mu_{2k}}$,

$$O = \sum_{\mu_1 \dots \mu_{2k}} o^{\mu_1 \dots \mu_k}_{\mu_{k+1} \dots \mu_{2k}} \bar{A}_{\mu_1} \dots \bar{A}_{\mu_k} A^{\mu_{k+1}} \dots A^{\mu_{2k}}. \quad (\text{A2})$$

In contrast, for applications to NCPT, it is more convenient to work with the fully covariant $(0, 2k)$ -tensor of coordinates $o_{\mu_1 \dots \mu_{2k}}$, which verify

$$O = \sum_{\mu_1 \dots \mu_{2k}} o_{\mu_1 \dots \mu_{2k}} A^{\mu_1} \dots A^{\mu_{2k}}. \quad (\text{A3a})$$

Conveniently choosing our Nambu fields to be related to the extended basis $\mathcal{B}^e = \mathcal{B} \cup \bar{\mathcal{B}}$, and using the definition of Nambu fields given in Eqs. (16), Eq. (A1) can be re-expressed as

$$O = \sum_{\substack{b_1 \dots b_k \\ c_1 \dots c_k}} o_{b_1 \dots b_k c_k \dots c_1} \bar{A}_{(b_1, 1)} \dots \bar{A}_{(b_k, 1)} A^{(c_1, 1)} \dots A^{(c_k, 1)}. \quad (\text{A4})$$

Therefore, we can easily relate $o_{b_1 \dots b_k c_1 \dots c_k}$ to the mixed representation matrix elements, $o^{\mu_1 \dots \mu_k}_{\mu_{k+1} \dots \mu_{2k}}$, accord-

ing to

$$o_{(b_1, l_1) \dots (b_k, l_k)} (c_1, m_1) \dots (c_k, m_k) = o_{b_1 \dots b_k c_1 \dots c_1} E_{l_1 m_1}^{11} \dots E_{l_k m_k}^{11}, \quad (\text{A5})$$

where the family E^{ij} denotes the canonical basis of 2×2 matrices, i.e.

$$E_{kl}^{ij} \equiv \delta_{ik} \delta_{jl}. \quad (\text{A6})$$

Let us recall that the metric in \mathcal{B}^e reads simply

$$g_{\mu\nu} = \delta_{\mu\bar{\nu}}. \quad (\text{A7})$$

Consequently, the fully covariant coordinates $o_{\mu_1 \dots \mu_{2k}}$ are related to the original matrix elements by the expression

$$o_{(b_1, l_1) \dots (b_k, l_k) (c_1, m_1) \dots (c_k, m_k)} = o_{b_1 \dots b_k c_1 \dots c_1} E_{l_1 m_1}^{21} \dots E_{l_k m_k}^{21}. \quad (\text{A8})$$

Notice that in Eqs. (A5) and (A8), the components of the tensor are separable between Nambu indices and single-particle indices.

Appendix B: Antisymmetrisation of vertices

In this appendix, we detail how totally and partially antisymmetric vertices arise in the Feynman rules given in Sec. III B. As an example, we then work out explicit expressions of antisymmetrised vertices in terms of standard single-particle matrix elements in the case of a two-body interaction.

1. Factorisation of un-symmetrised vertices

Let us consider the Feynman rules that are obtained in terms of un-symmetrised vertices. These can be obtained following, for instance, Chap. 5 of Ref. [58] by using Wick's theorem and recasting time-ordered integrals. Compared to Sec. III B, the only difference lies in the symmetry factor, which includes only considerations from permutation of vertices; and in the expressions of the vertices, which are not symmetrised. For a perturbation theory defined by the partitioning of Eq. (43), and a diagram \mathcal{G}_n with n vertices, the generic Feynman amplitude reads

$$\begin{aligned} \mathcal{A}_{\text{Unsymm}}^{\mu_1 \dots \mu_{2k}}(\tau_{\mu_1}, \dots, \tau_{\mu_{2k}}) &= \frac{(-1)^{n+L}}{S} \\ &\times \sum_{\lambda \dots \lambda} \frac{v_{\lambda \dots \lambda}^{(k_1)}}{(2k_1)!} \dots \frac{v_{\lambda \dots \lambda}^{(k_n)}}{(2k_n)!} \int_0^\beta d\tau_1 \dots d\tau_n \prod_{e \in I} -\mathcal{G}^{(0)\lambda\lambda}(\tau_i, \tau_j) \\ &\times \prod_{e \in E_{\text{in}}} -\mathcal{G}^{(0)\lambda\mu}(\tau_i, \tau_\mu) \prod_{e \in E_{\text{out}}} -\mathcal{G}^{(0)\mu\lambda}(\tau_\mu, \tau_j), \quad (\text{B1}) \end{aligned}$$

where we use the same generic notation as in Eq. (52). As mentioned earlier, there is no contribution to the

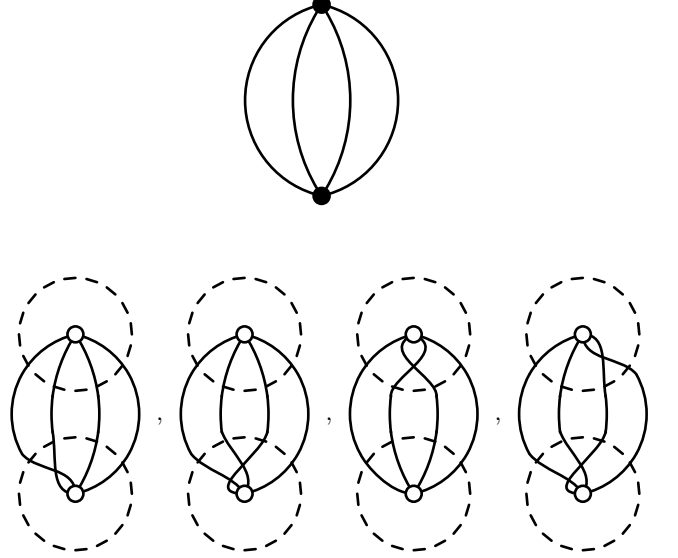


FIG. 8. Top: a second-order diagram \mathcal{G}_2^Z contributing to $\ln \frac{Z}{Z_0}$ which is expressed with fully antisymmetric vertices (filled dots). Bottom: four examples out of the 24 distinct diagrams in $\text{Sym}(\mathcal{G}_2^Z)$ expressed in terms of un-symmetrised vertices (empty dots). All diagrams are distinct only by their part within the dashed circles where half-lines are permuted.

symmetry factor coming from equivalent lines nor tadpoles and we work directly with the un-symmetrised vertices $\frac{1}{(2k)!} v_{\mu_1 \dots \mu_{2k}}^{(k)}$ appearing in the Hamiltonian. We represent these un-symmetrised vertices with an empty dot, in order to distinguish them from fully antisymmetrised ones that are represented with solid dots. Fig. 8 shows the example of a second-order diagram in the expansion of $\ln \frac{Z}{Z_0}$ with fully antisymmetric vertices (top) as well as several corresponding diagrams but with un-symmetrised vertices (bottom).

At this point, in a standard oriented diagrammatic, we would obtain its Hugenholtz version by using the antisymmetry of matrix elements with respect to exchange of outgoing and, separately, of incoming half-lines. This antisymmetry can be assumed without loss of generality thanks to the canonical anticommutation rules of creation and annihilation operators, namely Eqs. (2a) and (2b). To do so, we first define the set of oriented diagrams $\text{Hug}(\mathcal{G})$ made out of oriented diagrams \mathcal{G}' differing from an oriented diagram \mathcal{G} by permutations of incoming half-lines attached to a same vertex and (separately) of outgoing half-lines attached to a same vertex. Thanks to the assumed antisymmetry of matrix elements and the minus sign rule, the amplitude associated to any oriented diagram $\mathcal{G}' \in \text{Hug}(\mathcal{G})$ is the same as the one of \mathcal{G} , referred to as $\mathcal{A}_{\text{Unsymm}}$. Consequently, we can discard any contribution from oriented diagrams in $\text{Hug}(\mathcal{G})$ so long

as we associate the amplitude

$$\mathcal{A}_{\text{Hug}} \equiv \text{Card}(\text{Hug}(\mathcal{G})) \times \mathcal{A}_{\text{Unsymm}} \quad (\text{B2})$$

to \mathcal{G} , where $\text{Card}(\cdot)$ denotes the cardinal of a set. In practice, the Hugenholtz diagrammatic contributions are obtained directly from modified Feynman rules, which take into account the notion of equivalent lines. For more details on the Hugenholtz version of oriented diagrammatics we refer to standard textbooks on quantum many-body theory such as Ref. [58].

In the case of NCPT, the same procedure cannot be carried out so easily, because the tensors $v_{\mu_1 \dots \mu_{2k}}^{(k)}$ are in general *not* totally antisymmetric and the Nambu fields do not anticommute, namely

$$\{A^\mu, A^\nu\} = g^{\mu\nu} \neq 0. \quad (\text{B3})$$

To prove Eq. (52), which generalises the Hugenholtz antisymmetrisation, we use a different approach. We first define the set $\text{Sym}(\mathcal{G}_n)$ of un-oriented diagrams with n un-symmetrised vertices obtained from a given un-oriented diagram \mathcal{G}_n (also with un-symmetrised vertices) by any permutation of half-lines attached to a same vertex. Examples of un-oriented diagrams with un-symmetrised vertices which are obtained by this procedure are given at the bottom of Fig. 8. Let us emphasise that, compared to the previous Hugenholtz factorisation, we consider a larger set of permutations where *all* half-lines of a given vertex can be permuted. Without the antisymmetry of $v_{\mu_1 \dots \mu_{2k}}^{(k)}$, the amplitude associated to un-oriented diagrams in $\text{Sym}(\mathcal{G}_n)$ are not equal and we distinguish them by specifying a set of permutations (one for each vertex) denoted by $\sigma_1 \dots \sigma_n$. The sum of amplitudes of un-oriented diagrams in $\text{Sym}(\mathcal{G}_n)$ defines $\mathcal{A}^{\mu_1 \dots \mu_{2k}}(\tau_{\mu_1}, \dots, \tau_{\mu_{2k}})$ and reads

$$\mathcal{A}^{\mu_1 \dots \mu_{2k}}(\tau_{\mu_1}, \dots, \tau_{\mu_{2k}}) = \frac{1}{\prod_{l=2}^{l_{\max}} (l!)^m} \sum_{\sigma_1 \dots \sigma_n \in S_{2k_1} \times \dots \times S_{2k_n}} \mathcal{A}_{\text{Unsymm}}^{\mu_1 \dots \mu_{2k}}(\tau_{\mu_1}, \dots, \tau_{\mu_{2k}})[\sigma_1 \dots \sigma_n], \quad (\text{B4})$$

where $\mathcal{A}_{\text{Unsymm}}^{\mu_1 \dots \mu_{2k}}(\tau_{\mu_1}, \dots, \tau_{\mu_{2k}})[\sigma_1 \dots \sigma_n]$ denotes the amplitude associated to the un-oriented diagram obtained from \mathcal{G}_n by applying the half-line permutations $\sigma_1 \dots \sigma_n$ to its n vertices. The symmetry factor depends on equivalent lines, in such a way that it compensates for the double counting of un-oriented diagrams in $\text{Sym}(\mathcal{G}_n)$ when considering all permutations of half-lines $\sigma_1 \dots \sigma_n \in S_{2k_1} \times \dots \times S_{2k_n}$. Such double-counting is illustrated in Fig. 9 where the same un-oriented diagram is obtained with two different sets of permutations. For simplicity, we are assuming here that the un-oriented diagram \mathcal{G}_n is free of tadpoles. Following the labelling convention for vertices defined in Sec. III B, the amplitude $\mathcal{A}_{\text{Unsymm}}^{\mu_1 \dots \mu_{2k}}(\tau_{\mu_1}, \dots, \tau_{\mu_{2k}})[\sigma_1 \dots \sigma_n]$ of an un-oriented diagram obtained from \mathcal{G}_n with the permutations $\sigma_1 \dots \sigma_n$

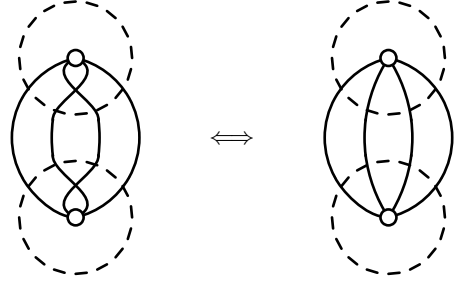


FIG. 9. Example of two different sets of permutations of half-lines which gives the same un-oriented diagram.

reads

$$\begin{aligned} \mathcal{A}_{\text{Unsymm}}^{\mu_1 \dots \mu_{2k}}(\tau_{\mu_1}, \dots, \tau_{\mu_{2k}})[\sigma_1 \dots \sigma_n] &= \frac{(-1)^{n+L}}{S} \\ &\times \sum_{\lambda \dots \lambda} \epsilon(\sigma_1) \frac{v_{\lambda \dots \lambda}^{(k_1)}}{(2k_1)!} \dots \epsilon(\sigma_n) \frac{v_{\lambda \dots \lambda}^{(k_n)}}{(2k_n)!} \\ &\times \int_0^\beta d\tau_1 \dots d\tau_n \prod_{e \in I} -\mathcal{G}^{(0)\lambda_\sigma \lambda_\sigma}(\tau_i, \tau_j) \\ &\times \prod_{e \in E_{\text{in}}} -\mathcal{G}^{(0)\lambda_\sigma \mu}(\tau_i, \tau_\mu) \prod_{e \in E_{\text{out}}} -\mathcal{G}^{(0)\mu \lambda_\sigma}(\tau_\mu, \tau_j), \quad (\text{B5}) \end{aligned}$$

where the signature of a permutation $\epsilon(\sigma_i)$ comes from extra crossing due to the permutations of half-lines of the i^{th} vertex and λ_σ denotes generically the modified global index, due to the permutations of half-lines of vertices, on which a propagator is contracted. Since the λ 's are dummy indices, we can perform the change of variables $\lambda_{\sigma_i} \leftarrow \lambda$ for indices attached to the i^{th} vertex (which amounts to renaming the half-lines of the i^{th} vertex) which leads to

$$\begin{aligned} \mathcal{A}_{\text{Unsymm}}^{\mu_1 \dots \mu_{2k}}(\tau_{\mu_1}, \dots, \tau_{\mu_{2k}})[\sigma_1 \dots \sigma_n] &= \frac{(-1)^{n+L}}{S} \\ &\times \sum_{\lambda \dots \lambda} \epsilon(\sigma_1) \frac{v_{\lambda_{\sigma_1^{-1}} \dots \lambda_{\sigma_1^{-1}}}^{(k_1)}}{(2k_1)!} \dots \epsilon(\sigma_n) \frac{v_{\lambda_{\sigma_n^{-1}} \dots \lambda_{\sigma_n^{-1}}}^{(k_n)}}{(2k_n)!} \\ &\times \int_0^\beta d\tau_1 \dots d\tau_n \prod_{e \in I} -\mathcal{G}^{(0)\lambda \lambda}(\tau_i, \tau_j) \\ &\times \prod_{e \in E_{\text{in}}} -\mathcal{G}^{(0)\lambda \mu}(\tau_i, \tau_\mu) \prod_{e \in E_{\text{out}}} -\mathcal{G}^{(0)\mu \lambda}(\tau_\mu, \tau_j), \quad (\text{B6}) \end{aligned}$$

where $v_{\lambda_{\sigma_i^{-1}} \dots \lambda_{\sigma_i^{-1}}}^{(k_i)}$ denotes the value $v_{\lambda \dots \lambda}^{(k_i)}$ where the indices have been permuted according to σ_i^{-1} . Plugging Eq. (B6) into Eq. (B4), and performing the change of variables $\sigma_i^{-1} \leftarrow \sigma_i$ we obtain the amplitude associated

to $\text{Sym}(\mathcal{G}_n)$, namely

$$\begin{aligned} \mathcal{A}^{\mu_1 \dots \mu_{2k}}(\tau_{\mu_1}, \dots, \tau_{\mu_{2k}}) = & \frac{1}{\prod_{l=2}^{l_{\max}} (l!)^m} \sum_{\sigma_1 \dots \sigma_n \in S_{2k_1} \times \dots \times S_{2k_n}} \frac{(-1)^{n+L}}{S} \\ & \times \sum_{\lambda \dots \lambda} \epsilon(\sigma_1) \frac{v_{\lambda_{\sigma_1} \dots \lambda_{\sigma_1}}^{(k_1)}}{(2k_1)!} \dots \epsilon(\sigma_n) \frac{v_{\lambda_{\sigma_n} \dots \lambda_{\sigma_n}}^{(k_n)}}{(2k_n)!} \\ & \times \int_0^\beta d\tau_1 \dots d\tau_n \prod_{e \in I} -\mathcal{G}^{(0)\lambda\lambda}(\tau_i, \tau_j) \\ & \times \prod_{e \in E_{\text{in}}} -\mathcal{G}^{(0)\lambda\mu}(\tau_i, \tau_\mu) \prod_{e \in E_{\text{out}}} -\mathcal{G}^{(0)\mu\lambda}(\tau_\mu, \tau_j), \quad (\text{B7}) \end{aligned}$$

where we have used the identity $\epsilon(\sigma^{-1}) = \epsilon(\sigma)$. The key point here is that the propagators appearing in Eq. (B7) do not explicitly depend on the permutations $\sigma_1, \dots, \sigma_n$, which allows us to factor them out of the sum over $\sigma_1, \dots, \sigma_n$. Assuming we can permute the sums over λ 's and over σ 's, we obtain

$$\begin{aligned} \mathcal{A}^{\mu_1 \dots \mu_{2k}}(\tau_{\mu_1}, \dots, \tau_{\mu_{2k}}) = & \frac{(-1)^{n+L}}{S \times \prod_{l=2}^{l_{\max}} (l!)^m} \\ & \times \sum_{\lambda \dots \lambda} \left(\frac{1}{(2k_1)!} \sum_{\sigma_1 \in S_{2k_1}} \epsilon(\sigma_1) v_{\lambda_{\sigma_1} \dots \lambda_{\sigma_1}}^{(k_1)} \right) \\ & \times \dots \times \left(\frac{1}{(2k_n)!} \sum_{\sigma_n \in S_{2k_n}} \epsilon(\sigma_n) v_{\lambda_{\sigma_n} \dots \lambda_{\sigma_n}}^{(k_n)} \right) \\ & \times \int_0^\beta d\tau_1 \dots d\tau_n \prod_{e \in I} -\mathcal{G}^{(0)\lambda\lambda}(\tau_i, \tau_j) \\ & \times \prod_{e \in E_{\text{in}}} -\mathcal{G}^{(0)\lambda\mu}(\tau_i, \tau_\mu) \prod_{e \in E_{\text{out}}} -\mathcal{G}^{(0)\mu\lambda}(\tau_\mu, \tau_j) \quad (\text{B8}) \end{aligned}$$

which is exactly Eq. (52) in the case where there are no tadpoles. Therefore, instead of summing amplitudes associated to un-oriented diagrams with un-symmetrised vertices, we sum over the distinct $\text{Sym}(\mathcal{G}_n)$ which are faithfully represented by un-oriented diagrams with the fully antisymmetric vertices defined in Eq. (50).

For an un-oriented diagram \mathcal{G}_n (with un-symmetrised vertices) that contains p_1, \dots, p_n tadpoles on its vertices, the derivation is similar. The only difference is in Eq. (B4), which we replace by

$$\begin{aligned} \mathcal{A}^{\mu_1 \dots \mu_{2k}}(\tau_{\mu_1}, \dots, \tau_{\mu_{2k}}) = & \frac{\prod_{i=1}^n 2^{p_i}}{2^T} \frac{\prod_{i=1}^n p_i!}{\prod_{l=2}^{l_{\max}} (l!)^m} \\ & \sum_{\substack{\sigma_1 \dots \sigma_n \\ \in (S_{2k_1}/S_2^{p_1} \times S_{p_1}) \\ \times \dots \times (S_{2k_n}/S_2^{p_n} \times S_{p_n})}} \mathcal{A}_{\text{Unsymm}}^{\mu_1 \dots \mu_{2k}}(\tau_{\mu_1}, \dots, \tau_{\mu_{2k}})[\sigma_1 \dots \sigma_n], \quad (\text{B9}) \end{aligned}$$

where $S_{2k}/S_2^p \times S_p$ denotes the set of permutations that do not permute half-lines inside tadpoles nor several tadpoles

between them. The term $p_i!$ appears in the numerator to compensate for the same term in the denominator coming from the p_i -tuple of equivalent lines making the p_i tadpoles on the i^{th} vertex. There is indeed no need to compensate double-counting in this case since the set of permutations, $S_{2k}/S_2^p \times S_p$, is already restricted to not contain any permutation exchanging tadpoles on a given vertex. The remaining factor does not modify the amplitude, because the total number of tadpoles is $T = p_1 + \dots + p_n$ so that

$$\frac{\prod_{i=1}^n 2^{p_i}}{2^T} = 1. \quad (\text{B10})$$

Similarly to the case without tadpoles, Eq. (B8) eventually reads

$$\begin{aligned} \mathcal{A}^{\mu_1 \dots \mu_{2k}}(\tau_{\mu_1}, \dots, \tau_{\mu_{2k}}) = & \frac{(-1)^{n+L}}{S \times 2^T \prod_{l=2}^{l_{\max}} (l!)^m} \\ & \times \sum_{\lambda \dots \lambda} \left(\frac{2^{p_1} p_1!}{(2k_1)!} \sum_{\sigma_1 \in S_{2k_1}/S_2^{p_1} \times S_{p_1}} \epsilon(\sigma_1) v_{\lambda_{\sigma_1} \dots \lambda_{\sigma_1}}^{(k_1)} \right) \\ & \times \dots \times \left(\frac{2^{p_n} p_n!}{(2k_n)!} \sum_{\sigma_n \in S_{2k_n}/S_2^{p_n} \times S_{p_n}} \epsilon(\sigma_n) v_{\lambda_{\sigma_n} \dots \lambda_{\sigma_n}}^{(k_n)} \right) \\ & \times \int_0^\beta d\tau_1 \dots d\tau_n \prod_{e \in I} -\mathcal{G}^{(0)\lambda\lambda}(\tau_i, \tau_j) \\ & \times \prod_{e \in E_{\text{in}}} -\mathcal{G}^{(0)\lambda\mu}(\tau_i, \tau_\mu) \prod_{e \in E_{\text{out}}} -\mathcal{G}^{(0)\mu\lambda}(\tau_\mu, \tau_j), \quad (\text{B11}) \end{aligned}$$

where the partial antisymmetrisation of vertices appears explicitly as defined in Eq. (51).

2. Antisymmetrised two-body interaction

We now proceed to explain how the fully antisymmetrised vertices of NCPT can be obtained from standard interaction matrix elements. Let us consider the perturbation theory defined by the partition

$$\Omega \equiv \Omega_0 + \Omega_1, \quad (\text{B12a})$$

$$\Omega_0 \equiv \frac{1}{2} \sum_{\mu\nu} U_{\mu\nu} A^\mu A^\nu, \quad (\text{B12b})$$

$$\Omega_1 \equiv \frac{1}{4!} \sum_{\mu_1 \mu_2 \mu_3 \mu_4} v_{\mu_1 \mu_2 \mu_3 \mu_4}^{(2)} A^{\mu_1} A^{\mu_2} A^{\mu_3} A^{\mu_4}, \quad (\text{B12c})$$

where only a pure two-body interaction contributes to the perturbation, and where the Nambu fields A^μ are left to be specified. Let \mathcal{B} be a single-particle basis. In the standard Gorkov formalism, the perturbation Ω_1 is expressed in terms of \bar{V}_{bcde} such that, in the basis \mathcal{B} ,

$$\Omega_1 = \frac{1}{(2!)^2} \sum_{bcde} \bar{V}_{bcde} \bar{a}_b \bar{a}_c a_e a_d. \quad (\text{B13})$$

Without loss of generality, \bar{V}_{bcde} is assumed to be partially antisymmetric, i.e.

$$\bar{V}_{bcde} = -\bar{V}_{cbde} = -\bar{V}_{bced} = \bar{V}_{cbde} . \quad (\text{B14})$$

It is convenient to work with the extended basis $\mathcal{B}^e = \mathcal{B} \cup \bar{\mathcal{B}}$, i.e. the contravariant Nambu fields read

$$A^{(b,1)} = a_b , \quad (\text{B15a})$$

$$A^{(b,2)} = \bar{a}_b . \quad (\text{B15b})$$

As discussed in App. A, the relation between $v_{\mu_1\mu_2\mu_3\mu_4}^{(2)}$ and \bar{V}_{bcde} reads

$$\frac{1}{3!} v_{[(b,l_b)(c,l_c)(d,l_d)(e,l_e)]}^{(2)} = \bar{V}_{bcde} E_{l_b l_e}^{21} E_{l_c l_d}^{21} , \quad (\text{B16})$$

where the $\frac{1}{3!}$ factor is due to a different normalisation in Eq. (B12c) and Eq. (B13).

In App. B1 we have shown why only the totally antisymmetric part of vertices contributes to the amplitude of an un-oriented Feynman diagram. In the case of vertices with tadpoles, a certain partial antisymmetrisation occurs instead. Regarding the totally antisymmetric part of $v_{\mu_1\mu_2\mu_3\mu_4}^{(2)}$, we use the symmetries in Eq. (B14) to simplify the $4!$ terms into a sum of only 6 terms, namely

$$\begin{aligned} v_{[(b,l_b)(c,l_c)(d,l_d)(e,l_e)]}^{(2)} &= \bar{V}_{bcde} E_{l_b l_e}^{21} E_{l_c l_d}^{21} + \bar{V}_{decb} E_{l_d l_c}^{21} E_{l_e l_b}^{21} \\ &\quad - \bar{V}_{bdec} E_{l_b l_e}^{21} E_{l_d l_c}^{21} - \bar{V}_{cedb} E_{l_c l_d}^{21} E_{l_e l_b}^{21} \\ &\quad + \bar{V}_{bedc} E_{l_b l_d}^{21} E_{l_e l_c}^{21} + \bar{V}_{cdeb} E_{l_c l_e}^{21} E_{l_d l_b}^{21} . \end{aligned} \quad (\text{B17})$$

Regarding partial antisymmetric parts of $v_{\mu_1\mu_2\mu_3\mu_4}^{(2)}$, we consider as an example $v_{[\mu_1\mu_2\mu_3\mu_4]}^{(2)}$ which appears in the first order expansion of the propagator given in Eq. (72). Similarly to Eq. (B17), we obtain a sum of 4 terms namely

$$\begin{aligned} v_{[(b,l_b)(c,l_c)(d,l_d)(e,l_e)]}^{(2)} &= 2\bar{V}_{bcde} E_{l_b l_e}^{21} E_{l_c l_d}^{21} \\ &\quad - 2\bar{V}_{cedb} E_{l_c l_d}^{21} E_{l_e l_b}^{21} \\ &\quad + \bar{V}_{bedc} E_{l_b l_d}^{21} E_{l_e l_c}^{21} + \bar{V}_{cdeb} E_{l_c l_e}^{21} E_{l_d l_b}^{21} . \end{aligned} \quad (\text{B18})$$

The above expressions of the totally and partially antisymmetric vertices are simple because of our choice of basis. We stress that this choice is arbitrary and might not be optimal for some specific applications. One may thus want to perform a change of extended basis. This is, however, very easily done thanks to the Nambu covariance of both $v_{[\mu_1\mu_2\mu_3\mu_4]}^{(2)}$ and $v_{[\mu_1\mu_2\mu_3\mu_4]}^{(2)}$.

Let us mention two common cases where the expressions simplify further. The first case consists in assuming the interaction potential to be Hermitian and having real-valued matrix elements. In this case, one can work with an orthonormal single-particle basis \mathcal{B} so that the Hermitian property reads

$$\bar{V}_{bcde}^* = \bar{V}_{decb} . \quad (\text{B19})$$

Combined with the realness assumption, the matrix elements verify

$$\bar{V}_{bcde} = \bar{V}_{decb} . \quad (\text{B20})$$

With this, the totally and partially antisymmetric parts of the vertices simplify, respectively, to

$$\begin{aligned} v_{[(b,l_b)(c,l_c)(d,l_d)(e,l_e)]}^{(2)} &= \bar{V}_{bcde} (E_{l_b l_e}^{21} E_{l_c l_d}^{21} + E_{l_d l_c}^{21} E_{l_e l_b}^{21}) \\ &\quad - \bar{V}_{bdec} (E_{l_b l_e}^{21} E_{l_d l_c}^{21} + E_{l_c l_d}^{21} E_{l_e l_b}^{21}) \\ &\quad + \bar{V}_{bedc} (E_{l_b l_d}^{21} E_{l_e l_c}^{21} + E_{l_c l_e}^{21} E_{l_d l_b}^{21}) , \end{aligned} \quad (\text{B21a})$$

$$\begin{aligned} v_{[(b,l_b)(c,l_c)(d,l_d)(e,l_e)]}^{(2)} &= 2\bar{V}_{bcde} E_{l_b l_e}^{21} E_{l_c l_d}^{21} \\ &\quad - 2\bar{V}_{cedb} E_{l_c l_d}^{21} E_{l_e l_b}^{21} \\ &\quad + \bar{V}_{bedc} (E_{l_b l_d}^{21} E_{l_e l_c}^{21} + E_{l_c l_e}^{21} E_{l_d l_b}^{21}) . \end{aligned} \quad (\text{B21b})$$

The second common simplification arises if we assume the potential to be Hermitian and time-reversal invariant. In this case, we again take \mathcal{B} to be orthonormal and the potential matrix elements verify Eq. (B19). To simplify the expressions of the antisymmetrised potential, it is now convenient to work in the extended basis $\mathcal{B}^{e\prime} = \mathcal{B} \cup \bar{\mathcal{B}}^\dagger$, where $\bar{\mathcal{B}}$ is the orthonormal single-particle basis obtained from \mathcal{B} by applying the time-reversal operator. In this case, time-reversal invariance implies

$$\bar{V}_{bcde}^* = \bar{V}_{\bar{b}\bar{c}\bar{d}\bar{e}} , \quad (\text{B22})$$

where $\bar{V}_{\bar{b}\bar{c}\bar{d}\bar{e}}$ denotes the matrix elements of the potential in the $\bar{\mathcal{B}}$ single-particle basis. Combined with the Hermitian property of Eq. (B19), the matrix elements verify

$$\bar{V}_{bcde} = \bar{V}_{\bar{d}\bar{e}\bar{b}\bar{c}} . \quad (\text{B23})$$

Then, performing a non-canonical change of extended basis to go from \mathcal{B}^e to $\mathcal{B}^{e\prime}$ and using Eq. (B23), we obtain

$$\begin{aligned} v_{[(b,l_b)(c,l_c)(d,l_d)(e,l_e)]}^{(2)} &= \bar{V}_{\bar{b}\bar{c}\bar{e}\bar{d}} (E_{l_b l_e}^{21} E_{l_c l_d}^{21} + E_{l_d l_c}^{21} E_{l_e l_b}^{21}) \\ &\quad - \bar{V}_{\bar{b}\bar{d}\bar{e}\bar{c}} (E_{l_b l_e}^{21} E_{l_d l_c}^{21} + E_{l_c l_d}^{21} E_{l_e l_b}^{21}) \\ &\quad + \bar{V}_{\bar{b}\bar{e}\bar{d}\bar{c}} (E_{l_b l_d}^{21} E_{l_e l_c}^{21} + E_{l_c l_e}^{21} E_{l_d l_b}^{21}) , \end{aligned} \quad (\text{B24a})$$

$$\begin{aligned} v_{[(b,l_b)(c,l_c)(d,l_d)(e,l_e)]}^{(2)} &= 2\bar{V}_{\bar{b}\bar{c}\bar{e}\bar{d}} E_{l_b l_e}^{21} E_{l_c l_d}^{21} \\ &\quad - 2\bar{V}_{\bar{c}\bar{e}\bar{d}\bar{b}} E_{l_c l_d}^{21} E_{l_e l_b}^{21} \\ &\quad + \bar{V}_{\bar{b}\bar{e}\bar{d}\bar{c}} (E_{l_b l_d}^{21} E_{l_e l_c}^{21} + E_{l_c l_e}^{21} E_{l_d l_b}^{21}) . \end{aligned} \quad (\text{B24b})$$

These expressions are very similar to Eqs. (B21), but now include matrix elements between single-particle states and their time-reversal.

Appendix C: Gaudin's rules for a general diagram

In Sec. III D, we discussed Gaudin's summation rules for evaluating the Matsubara frequency sums appearing

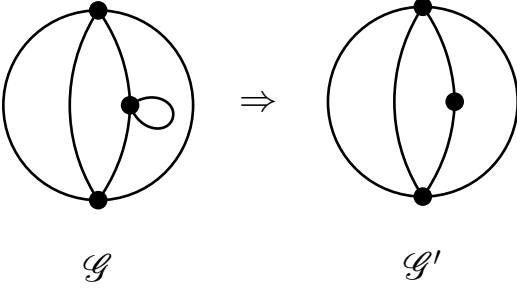


FIG. 10. Example of a 3rd order diagram \mathcal{G} containing a tadpole (left), together with its associated diagram \mathcal{G}' obtained by stripping tadpoles (right).

in the algebraic expression of diagrams in the energy representation. To be concise, we focused on connected diagrams without tadpoles nor external lines. We now proceed to discuss the required extensions to evaluate the sums for any diagram.

1. Extension to tadpoles

Let \mathcal{G} be a connected un-oriented Feynman diagram without external lines. If \mathcal{G} contains tadpoles, we can still apply the same set of Gaudin's summation rules described in Sec. III D, so long as we perform an intermediate pre-processing step. This step consists simply in analytically performing the sum over Matsubara frequencies stemming from each tadpole. For any given tadpole, the Matsubara sum is performed explicitly by applying the identity

$$\frac{1}{\beta} \sum_{\omega_t} \mathcal{G}^{(0)\mu_t\nu_t}(\omega_t) e^{-i\omega_t\eta} = \sum_{n_t} f(-\epsilon_{n_t}) X^{(n_t)\mu_t} \bar{X}^{(n_t)\nu_t}, \quad (\text{C1})$$

where ω_t are Matsubara frequencies; ϵ_{n_t} , quasiparticle energies; and μ_t and ν_t , global indices associated to the tadpole t .

Having performed the tadpole Matsubara sums, we still need to evaluate the remaining contributions in the sum. One can do this by applying Gaudin's summation rules to the diagram \mathcal{G}' , obtained from \mathcal{G} by stripping all of its tadpole lines. Explicitly, the result of the Matsubara sums in \mathcal{G} , $I(\mathcal{G})$, is related to the full sums in \mathcal{G}' , $I(\mathcal{G}')$, by

$$I(\mathcal{G}) = \prod_{t \in T} \left(\sum_{n_t} f(-\epsilon_{n_t}) X^{(n_t)\mu_t} \bar{X}^{(n_t)\nu_t} \right) \times I(\mathcal{G}'), \quad (\text{C2})$$

where t indexes all the tadpoles T in \mathcal{G} and n_t indexes quasiparticle energies associated to the tadpole t . We illustrate the transformation from a diagram \mathcal{G} to a tadpole-free diagram \mathcal{G}' in Fig. 10. With Eq. (C2), Gaudin's summation rules are extended to any connected diagram without external lines.

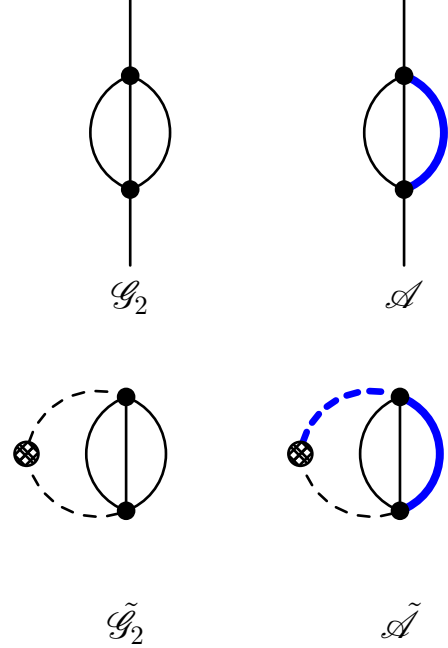


FIG. 11. Top left: a second order diagram \mathcal{G}_2 with two external lines. Top right: one spanning tree \mathcal{A} of \mathcal{G}_2 . Bold blue lines represent lines belonging to \mathcal{A} . Bottom left: the associated diagram $\tilde{\mathcal{G}}_2$. The hatched vertex represents v_{fix} . Dashed lines represent the contractions to v_{fix} . Bottom right: the modified spanning tree $\tilde{\mathcal{A}}$. The dashed bold blue line represents e_{fix} .

2. Extension to external lines

Let us now consider a connected diagram \mathcal{G} with $2k$ external lines. We consider, without loss of generality, that \mathcal{G} does not contain any tadpole. If it does, one can use the pre-processing step and results in the previous subsection to evaluate their contribution.

We can incorporate the presence of external lines in Gaudin's summation rules to the price of some minor modifications, which we enumerate now. Rules 1. and 2. of Sec. III D are still valid, but with the additional restriction that spanning trees, as well as their complementary diagrams, must only be made of internal lines.

Rule 3.a. remains the same. The generalisation of rule 3.b. is slightly more involved. As discussed in Sec. III C, the global conservation of energy fixes one Matsubara frequency among the $2k$ (external) possible frequencies. The line associated to the energy fixed by global conservation of energy is denoted as e_{fix} . Let \mathcal{A} be a spanning tree (made only of internal lines) of \mathcal{G} . The modified 3.b. rule reads

3.b.' Consider the diagram $\tilde{\mathcal{G}}$ made of \mathcal{G} plus an additional vertex v_{fix} with all external lines contracted to it. Consider the spanning tree $\tilde{\mathcal{A}}$ of $\tilde{\mathcal{G}}$ made of \mathcal{A} , v_{fix} and e_{fix} . The denominator associated to line a of $\tilde{\mathcal{A}}$ is the one obtained by the original rule 3.b. when applied to line a of $\tilde{\mathcal{A}}$ in $\tilde{\mathcal{G}}$.

Modified diagrams and spanning trees stemming from rule 3.b.' are illustrated in Fig. 11.

Finally, we need to consider the extension of rule 3.c. In this case, it suffices to distinguish between internal and external lines, so that rule 3.c. is replaced by

3.c.' For each *internal* line e in \mathcal{G} multiply by a factor $X^{(n_e)\mu_e} \bar{X}^{(n_e)\nu_e}$. For each *external* line, multiply simply by a propagator as in the Feynman rules.

If the diagram must be expressed in terms of spectroscopic amplitudes only, we just have to replace all external propagators by their spectral representation using Eqs. (61) and (62).

3. Extension to disconnected diagrams

With the extensions given in Secs. C1 and C2, Gaudin's summation rules can now be applied to any connected

diagram. For completeness, we now turn to the case of disconnected diagrams. Let \mathcal{G} be a disconnected diagram, with $\Gamma_1 \dots \Gamma_C$ its C distinct connected parts. Since the sub-diagrams $\Gamma_1 \dots \Gamma_C$ do not share any vertices nor lines, the Matsubara frequencies of each connected parts are necessarily independent. The global Matsubara sum can thus be factorised, so that

$$I(\mathcal{G}) = \prod_{i=1}^C I(\Gamma_i). \quad (\text{C3})$$

Since each Γ_i is a connected diagram, we can apply Gaudin's summation rules (or their extension if Γ_i contains external lines or tadpoles) to compute each term $I(\Gamma_i)$.

With the tadpole, external line and disconnected extensions just discussed, Gaudin's summation rules introduced in Sec. IIID can be applied to any diagram.

-
- [1] J. Bardeen, L. N. Cooper, and J. R. Schrieffer, *Phys. Rev.* **106**, 162 (1957).
 - [2] J. Bardeen, L. N. Cooper, and J. R. Schrieffer, *Phys. Rev.* **108**, 1175 (1957).
 - [3] N. N. Bogoliubov, *Sov. Phys. JETP* **7**, 41 (1958).
 - [4] L. Gor'kov, *Sov. Phys. JETP* **7**, 158 (1958).
 - [5] V. Soma, T. Duguet, and C. Barbieri, *Phys. Rev. C* **84**, 064317 (2011).
 - [6] A. Signoracci, T. Duguet, G. Hagen, and G. R. Jansen, *Phys. Rev. C* **91**, 064320 (2015).
 - [7] J. Valatin, *Nuovo Cimento* **7**, 843 (1958).
 - [8] V. Tolmachev, S. Tiablikov, and J. Exptl, *Sov. Phys. JETP* **7**, 46 (1958).
 - [9] N. N. Bogoliubov, *Sov. Phys. JETP* **7**, 51 (1958).
 - [10] P. W. Anderson, *Phys. Rev.* **112**, 1900 (1958).
 - [11] Y. Nambu, *Phys. Rev.* **117**, 648 (1960).
 - [12] R. D. Mattuck, *A guide to Feynman diagrams in the many-body problem* (McGraw-Hill, New York, NY, 1976).
 - [13] C. De Dominicis and P. C. Martin, *J. Math. Phys.* **5**, 14 (1964).
 - [14] C. De Dominicis and P. C. Martin, *J. Math. Phys.* **5**, 31 (1964).
 - [15] H. Kleinert, *Lett. Nuovo Cimento* **31**, 521 (1981).
 - [16] H. Kleinert, *Fortschr. Phys.* **30**, 351 (1982).
 - [17] R. Haussmann, *Z. Phys. B* **91**, 291 (1993).
 - [18] R. Haussmann, *Self-consistent quantum-field theory and bosonization for strongly correlated electron systems* (Springer, Berlin, Heidelberg, 1999).
 - [19] P. Curie, *J. Phys. Theor. Appl.* **3**, 393 (1894).
 - [20] P. W. Anderson, *Science* **177**, 393 (1972).
 - [21] P. Ring and P. Schuck, *The Nuclear Many-Body Problem* (Springer, Berlin, Heidelberg, 1980).
 - [22] D. Pines and M. A. Alpar, *Nature* **316**, 27 (1985).
 - [23] T. Takatsuka and R. Tamagaki, *Prog. Theo. Phys. Suppl.* **112**, 27 (1993).
 - [24] R. Tamagaki, *Prog. Theo. Phys.* **44**, 905 (1970).
 - [25] M. Hoffberg, A. E. Glassgold, R. W. Richardson, and M. Ruderman, *Phys. Rev. Lett.* **24**, 775 (1970).
 - [26] M. Baldo, O. Elgarøy, L. Engvik, M. Hjorth-Jensen, and H.-J. Schulze, *Phys. Rev. C* **58**, 1921 (1998).
 - [27] D. J. Dean and M. Hjorth-Jensen, *Rev. Mod. Phys.* **75**, 607 (2003).
 - [28] A. Schwenk and B. Friman, *Phys. Rev. Lett.* **92**, 082501 (2004).
 - [29] V. A. Khodel, J. W. Clark, M. Takano, and M. V. Zverev, *Phys. Rev. Lett.* **93**, 151101 (2004).
 - [30] D. Ding, A. Rios, H. Dussan, W. H. Dickhoff, S. J. Witte, A. Carbone, and A. Polls, *Phys. Rev. C* **94**, 025802 (2016).
 - [31] C. Drischler, T. Krüger, K. Hebeler, and A. Schwenk, *Phys. Rev. C* **95**, 024302 (2017).
 - [32] A. Rios, A. Polls, and W. H. Dickhoff, *J. Low Temp. Phys.* **189**, 234 (2017).
 - [33] D. Yakovlev and C. Pethick, *Annu. Rev. Astron. Astrophys.* **42**, 169 (2004).
 - [34] D. Page and J. H. Applegate, *Astrophys. J.* **394**, L17 (1992).
 - [35] D. Yakovlev, O. Gnedin, A. Kaminker, K. Levenfish, and A. Potekhin, *Adv. Space Res.* **33**, 523 (2004).
 - [36] D. Blaschke, H. Grigorian, and D. N. Voskresensky, *Phys. Rev. C* **88**, 065805 (2013).
 - [37] K. Hebeler, J. Holt, J. Menéndez, and A. Schwenk, *Annu. Rev. Nucl. Part. Sci.* **65**, 457 (2015).
 - [38] A. Rios, *Front. Phys. (Lausanne)* **8**, 387 (2020).
 - [39] C. Drischler, K. Hebeler, and A. Schwenk, *Phys. Rev. Lett.* **122**, 042501 (2019).
 - [40] C. Drischler, J. W. Holt, and C. Wellenhofer, *Annu. Rev. Nucl. Part. Sci.* **71** (2021), 10.1146/annurev-nucl-102419-041903.
 - [41] C. Shen, U. Lombardo, and P. Schuck, *Phys. Rev. C* **71**, 054301 (2005).
 - [42] V. Somà, *Front. Phys. (Lausanne)* **8**, 340 (2020).
 - [43] V. Somà, P. Navrátil, F. Raimondi, C. Barbieri, and T. Duguet, *Phys. Rev. C* **101**, 014318 (2020).
 - [44] C. Barbieri and A. Carbone, "Self-consistent green's function approaches," in *An Advanced Course in Computa-*

- tional Nuclear Physics: Bridging the Scales from Quarks to Neutron Stars*, edited by M. Hjorth-Jensen, M. P. Lombardo, and U. van Kolck (Springer International Publishing, Cham, 2017) pp. 571–644.
- [45] A. Carbone, A. Cipollone, C. Barbieri, A. Rios, and A. Polls, *Phys. Rev. C* **88**, 054326 (2013).
- [46] F. Raimondi and C. Barbieri, *Phys. Rev. C* **97**, 054308 (2018).
- [47] P. D. Stevenson, *Int. J. Mod. Phys. C* **14**, 1135 (2003).
- [48] P. Arthuis, T. Duguet, A. Tichai, R.-D. Lasserri, and J.-P. Ebran, *Comput. Phys. Commun.* **240**, 202 (2019).
- [49] A. Tichai, R. Wirth, J. Ripoché, and T. Duguet, *Eur. Phys. J. A* **56**, 272 (2020).
- [50] V. Somà, C. Barbieri, and T. Duguet, *Phys. Rev. C* **89**, 024323 (2014).
- [51] T. Duguet and A. Signoracci, *J. Phys. G* **44**, 015103 (2016).
- [52] O. Sinanoğlu, *Theor. Chim. Acta* **65**, 233 (1984).
- [53] M. Head-Gordon, P. E. Maslen, and C. A. White, *J. Chem. Phys.* **108**, 616 (1998).
- [54] M. Drissi, A. Rios, and C. Barbieri, “Nambu-Covariant Many-Body Theory II: Self-Consistent Approximations,” (2021).
- [55] J. Dongarra, M. Gates, A. Haidar, J. Kurzak, P. Luszczek, S. Tomov, and I. Yamazaki, “Accelerating Numerical Dense Linear Algebra Calculations with GPUs,” in *Numerical Computations with GPUs*, edited by V. Kindratenko (Springer International Publishing, Cham, 2014) pp. 3–28.
- [56] M. Gates, J. Kurzak, A. Charara, A. YarKhan, and J. Dongarra, in *Proceedings of the International Conference for High Performance Computing, Networking, Storage and Analysis*, SC '19 (Association for Computing Machinery, New York, NY, USA, 2019).
- [57] R. Balian and E. Brezin, *Nuovo Ciment. B* **64**, 37 (1969).
- [58] J.-P. Blaizot and G. Ripka, *Quantum theory of finite systems* (MIT Press, Cambridge, Massachusetts, 1986).
- [59] G. Stefanucci and R. van Leeuwen, *Nonequilibrium Many-Body Theory of Quantum Systems: A Modern Introduction* (Cambridge University Press, 2013).
- [60] M. Gaudin, *Nucl. Phys.* **15**, 89 (1960).
- [61] P. Nozières, *Theory of interacting Fermi systems* (Addison-Wesley, 1964).
- [62] M. Gaudin, *Nuovo Cimento* **38**, 844 (1965).
- [63] F. Guerin, *Phys. Rev. D* **49**, 4182 (1994).
- [64] C. Dib, O. Espinosa, and I. Schmidt, *Phys. Lett. B* **402**, 147 (1997).
- [65] S. M. H. Wong, *Phys. Rev. D* **64**, 025007 (2001).
- [66] O. Espinosa and E. Stockmeyer, *Phys. Rev. D* **69**, 065004 (2004).
- [67] J.-P. Blaizot and U. Reinosa, *Nucl. Phys. A* **764**, 393 (2006).
- [68] U. Reinosa, *Renormalisation d'un schéma d'approximation auto-cohérent en théorie des champs à température finie*, Ph.D. thesis, CEA/Saclay/SPhT, École Polytechnique (2004), 2004EPXX0060.
- [69] J. W. Negele and H. Orland, *Quantum Many-Particle Systems* (Addison-Wesley, 1987).
- [70] A. Tichai, P. Arthuis, T. Duguet, H. Hergert, V. Somà, and R. Roth, *Phys. Lett. B* **786**, 195 (2018).
- [71] B. Nagy and F. Jensen, “Basis sets in quantum chemistry,” in *Reviews in Computational Chemistry* (John Wiley and Sons, 2017) Chap. 3, pp. 93–149.
- [72] M. A. Caprio, P. Maris, and J. P. Vary, *Phys. Rev. C* **86**, 034312 (2012).
- [73] A. Tichai, J. Müller, K. Vobig, and R. Roth, *Phys. Rev. C* **99**, 034321 (2019).
- [74] J. Hoppe, A. Tichai, M. Heinz, K. Hebeler, and A. Schwenk, *Phys. Rev. C* **103**, 014321 (2021).
- [75] Z. Rolik, A. Szabados, and P. R. Surján, *J. Chem. Phys.* **119**, 1922 (2003).
- [76] A. Tichai, E. Gebrerufael, K. Vobig, and R. Roth, *Phys. Lett. B* **786**, 448 (2018).
- [77] H. G. A. Burton and A. J. W. Thom, *J. Chem. Theory Comput.* **16**, 5586 (2020).
- [78] H. Feshbach, *Ann. Phys. (N. Y.)* **19**, 287 (1962).
- [79] Y. Ashida, Z. Gong, and M. Ueda, *Adv. Phys.* **69**, 249 (2020).